Article

Cell Reports

miRNAs Are Essential for the Regulation of the PI3K/AKT/FOXO Pathway and Receptor Editing during B Cell Maturation

Graphical Abstract

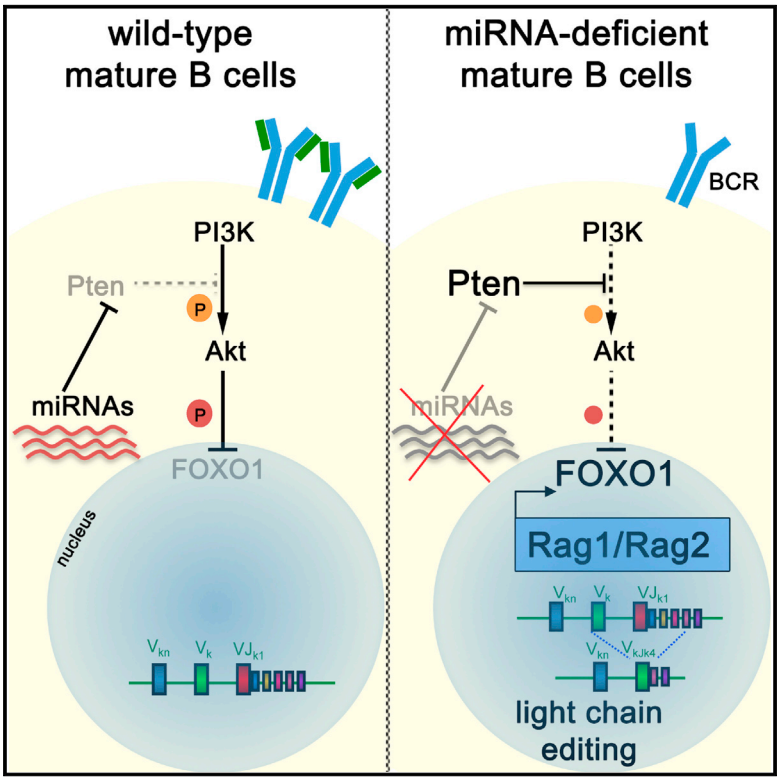

Authors

Maryaline Coffre, David Benhamou, David Rieß, ..., Jane A. Skok, Klaus Rajewsky, Sergei B. Koralov

Correspondence

sergei.koralov@nyumc.org

In Brief

Using mice in which RNAi is abolished selectively in B cells, Coffre et. al. demonstrate that miRNAs are essential for the regulation of the PI3K/AKT/FOXO1 pathway. The authors then demonstrate that PI3K signaling plays a critical role in the regulation of RAG expression and immunoglobulin light chain recombination in mature B lymphocytes.

Highlights

- Dicer-/Drosha-/DGCR8-dependent ncRNAs are essential for pre-B survival and proliferation
- Dicer- and DGCR8-dependent miRNAs control the PI3K/AKT/FOXO1 pathway in B cells
- Regulation of PI3K signaling by miRNAs is essential for keeping Rag expression in check
- Loss of miRNAs in peripheral B cells leads to immunoglobulin light chain editing

Coffre et al., 2016, Cell Reports *17*, 2271–2285
November 22, 2016
http://dx.doi.org/10.1016/j.celrep.2016.11.006

CellPress

Cell Reports
Article

miRNAs Are Essential for the Regulation of the PI3K/AKT/FOXO Pathway and Receptor Editing during B Cell Maturation

Maryaline Coffre,[1] David Benhamou,[2] David Rieß,[3,8] Lili Blumenberg,[1] Valentina Snetkova,[1] Marcus J. Hines,[1] Tirtha Chakraborty,[3,9] Sofia Bajwa,[1] Kari Jensen,[3] Mark M.W. Chong,[4,10] Lelise Getu,[5] Gregg J. Silverman,[1,5] Robert Blelloch,[6] Dan R. Littman,[4,7] Dinis Calado,[3,11] Doron Melamed,[2] Jane A. Skok,[1] Klaus Rajewsky,[3,12] and Sergei B. Koralov[1,13,*]

[1]Department of Pathology, New York University School of Medicine, New York, NY 10016, USA
[2]Department of Immunology, Faculty of Medicine, Technion, Haifa 31096, Israel
[3]Harvard Medical School, Pathology, Boston, MA 02115, USA
[4]Skirball Institute, NYU School of Medicine, New York, NY 10016, USA
[5]Department of Medicine, NYU School of Medicine, New York, NY 10016, USA
[6]Department of Urology, UCSF, San Francisco, CA 94143, USA
[7]The HHMI, NYU School of Medicine, New York, NY 10016, USA
[8]Present address: Hematology and Oncology, Technische Universität München, 81675 Munich, Germany
[9]Present address: CRISPR Therapeutics, Cambridge, MA 02139, USA
[10]Present address: St. Vincent's Institute of Medical Research, University of Melbourne, Fitzroy, Australia
[11]Present address: Immunity and Cancer Laboratory, The Francis Crick Institute, London NW1 1AT, UK
[12]Present address: Immune Regulation and Cancer, Max Delbrück Center for Molecular Medicine, 13125 Berlin, Germany
[13]Lead Contact
*Correspondence: sergei.koralov@nyumc.org
http://dx.doi.org/10.1016/j.celrep.2016.11.006

SUMMARY

B cell development is a tightly regulated process dependent on sequential rearrangements of immunoglobulin loci that encode the antigen receptor. To elucidate the role of microRNAs (miRNAs) in the orchestration of B cell development, we ablated all miRNAs at the earliest stage of B cell development by conditionally targeting the enzymes critical for RNAi in early B cell precursors. Absence of any one of these enzymes led to a block at the pro- to pre-B cell transition due to increased apoptosis and a failure of pre-B cells to proliferate. Expression of a Bcl2 transgene allowed for partial rescue of B cell development, however, the majority of the rescued B cells had low surface immunoglobulin expression with evidence of ongoing light chain editing. Our analysis revealed that miRNAs are critical for the regulation of the PTEN-AKT-FOXO1 pathway that in turn controls Rag expression during B cell development.

INTRODUCTION

MicroRNAs (miRNAs) are small (~22 nucleotides) endogenous non-coding RNAs (ncRNAs) that regulate gene expression by a process known as RNAi. RNAi is an evolutionary conserved mechanism regulating many physiological processes such as development, cell differentiation, proliferation, and survival (Castel and Martienssen, 2013; Pauli et al., 2011; Wilson and Doudna, 2013).

miRNA genes are transcribed by RNA polymerase II into double-stranded hairpin primary miRNAs (pri-miRNAs). The microprocessor composed of the ribonuclease (RNase) III Drosha and the double stranded RNA binding protein DiGeorge critical region 8 (DGCR8) cut the pri-miRNAs into shorter stem-loop precursor miRNAs (pre-miRNAs). Pre-miRNAs are exported from the nucleus into the cytoplasm, where they are further cleaved by the RNase III Dicer into 20–23 nucleotides miRNAs duplexes. The mature miRNA, is then incorporated into the RNA-induced silencing complex (RISC) and guides the complex to the 3′UTR of target mRNAs, leading to degradation and/or translational inhibition of the target mRNA (Krol et al., 2010; Wilson and Doudna, 2013; Winter et al., 2009). In vertebrates, hundreds of miRNA genes have been identified and more are predicted by computational analysis with each miRNA capable of regulating gene expression of numerous target genes (Lim et al., 2003, 2005).

In addition to the canonical miRNAs, which depend on Drosha, DGCR8, and Dicer for their biogenesis, other ncRNAs have been described that differ in their requirement for Dicer or the microprocessor complex (Okamura and Lai, 2008). Among these ncRNAs are miRNAs that are independent of Dicer, endogenous transposons, small nucleolar RNAs, endogenous small interfering RNAs, mirtrons produced by splicing, and long ncRNAs (Babiarz et al., 2008; Ender et al., 2008; Ruby et al., 2007; Seong et al., 2014). The function, processing, and regulation of many of these classes of ncRNAs in mammals remain to be fully elucidated.

B lymphocytes develop in the bone marrow (BM) through a tightly regulated process resulting in expression of a functional and unique B cell receptor (BCR) on the cell surface. The BCR is composed of a membrane bound antibody together with the signal transducing immunoglobulin (Ig) α and β subunits. Diversity of BCRs is achieved through somatic V(D)J rearrangements at the Ig heavy (IgH) and light (IgL) chain loci, mediated by the recombination activating genes (RAG) 1 and 2. Following IgH and IgL rearrangements at the pro-B and pre-B cell stage, respectively, immature B cells expressing a the newly minted BCR on their surface leave the bone marrow and enter circulation (Rajewsky, 1996). Despite being extensively studied, our understanding of B cell development remains fragmentary (Busslinger, 2004; Peled et al., 2008; Stavnezer et al., 2008).

Recently, there has been growing interest in the possible role of small ncRNAs in B cell development and function. The differential expression of miRNAs throughout B cell development suggests that these ncRNAs contribute to stage-specific regulation of the intricate transcriptional program during B cell development (Kuchen et al., 2010; Spierings et al., 2011). Indeed, conditional ablation of Dicer at different stages of B cell development reveals a critical role of Dicer-dependent ncRNAs in pre-B cells, follicular, and germinal center B cells (Belver et al., 2010; Koralov et al., 2008; Xu et al., 2012). These studies, as well as several investigations into the role of individual miRNAs throughout B cell development (Benhamou et al., 2016; Chen et al., 2004; Fragoso et al., 2012; Gonzalez-Martin et al., 2016; Koralov et al., 2008; Lai et al., 2016; Rao et al., 2010; Ventura et al., 2008; Xiao et al., 2007; Zhou et al., 2007), suggest that miRNAs are important for choreographing the expression of the various transcription factors and other key components controlling the different stages of B cell development and function. Several miRNAs that have been shown to be important in B cells are deregulated in B cell lymphomas (Di Lisio et al., 2012; He et al., 2005; Mu et al., 2009; Xiao et al., 2008) suggesting a role of miRNAs in B cell lymphomagenesis both in human and mouse. Although these studies demonstrate a critical role for miRNAs in the regulation of B cell development and function, they do not provide a complete picture of the role of miRNAs in B cell differentiation, because they do not take into account the fact that different miRNAs can act in concert to regulate a given signaling pathway. A more global approach is therefore necessary.

In the present study, we compare the phenotypes of mice in which *Dicer*, *Drosha*, or *Dgcr8* are conditionally ablated in the B cell lineage. Phenotypic changes observed upon conditional ablation of Dicer may be mediated not just by the Dicer-dependent miRNAs, but other Dicer-dependent ncRNAs. Analysis of B lymphocytes lacking components of the microprocessor complex (*Drosha* or *DGCR8*) allow us to unequivocally identify the impact of miRNA loss. Conditional deletion of either *Dicer*, *Drosha*, or *Dgcr8* led to an early block in B cell development due to increased cell death and decreased proliferation at the pre-B stage. Rescue of B cell development by overexpression of the anti-apoptotic factor Bcl2 revealed that in the absence of these enzymes critical to miRNA biogenesis, B lineage cells in the periphery expressed low surface levels of Ig heavy chains without expressing light chains. Furthermore, because the phenotype of the Drosha- and DGCR8-deficient B cells mirrored that of Dicer null B cells, we conclude the regulation of gene expression by miRNA was central to this phenotype. As a consequence of miRNA loss the phosphatidylinositol 3-kinase (PI3K)/AKT pathway was downregulated in the mutant cells through upregulation of phosphatase and tensin homolog (PTEN), leading to inappropriate RAG1 and RAG2 expression and continuous light chain editing. Our data suggest a critical role for miRNAs in the maintenance of a mature phenotype in peripheral B cells.

RESULTS

Drosha, DGCR8, and Dicer Deficiency Results in a Similar Block of B Cell Development at an Early Stage

We have previously demonstrated that *Dicer1*$^{fl/fl}$ *Mb1*-cre mice present a severe defect in B cell development (Koralov et al., 2008). To investigate whether the impaired B cell development was due to the lack of miRNAs or to absence of other ncRNAs, we crossed mice harboring conditional alleles for *Dgcr8* (Wang et al., 2007) or *Drosha* (Chong et al., 2008) with *Mb1*-cre animals (Hobeika et al., 2006). In these mice, *Dgcr8* or *Drosha* are deleted at the earliest stage of B cell development. In *Dgcr8*$^{fl/fl}$ *Mb1*-cre mice, pro-B cells (B220^{+}IgM^{-}c-kit^{+}) accumulated whereas only few pre-B cells (B220^{+}IgM^{-}CD25^{+}) were present. Immature (B220^{Int}IgM^{+}) and recirculating (B220^{Hi}IgM^{+}) B cells were largely absent in the bone marrow of these mice (Figures 1A and S1A). Consistent with the complementary role of DGCR8 and Drosha in the microprocessor complex, the block in B cell development in *Drosha*$^{fl/fl}$ *Mb1*-cre mice closely resembled that observed in *Dgcr8*$^{fl/fl}$ *Mb1*-cre animals (Figures S1A and S1B). This block at the pro-B to pre-B transition in *Dgcr8*$^{fl/fl}$ *Mb1*-cre and *Drosha*$^{fl/fl}$ *Mb1*-cre mice recapitulated the B cell developmental defect observed in *Dicer1*$^{fl/fl}$ *Mb1*-cre mice (Koralov et al., 2008). This suggested that ncRNAs processed by DGCR8, Drosha, and Dicer, most probably miRNAs, are critical for the transition from the pro- to the pre-B cell stage.

Annexin V staining revealed a striking increase in apoptotic pre-B, but not pro-B cells, in *Dgcr8*$^{fl/fl}$ *Mb1*-cre and *Drosha*$^{fl/fl}$ *Mb1*-cre mice compared to controls (Figures 1B and S2A). We have previously described upregulation of Bim upon deletion of Dicer in pre-B cells (Koralov et al., 2008), and B lymphocytes deficient for the miR-17$\sim$92 family members also exhibited higher level of this pro-apoptotic Bcl2 family member (Ventura et al., 2008). Consistent with the global loss of miRNAs in these cells, pro-B and pre-B cells from the bone marrow of *Dgcr8*$^{fl/fl}$ *Mb1*-cre (Figure 1C) or *Drosha*$^{fl/fl}$ *Mb1*-cre (Figure S2B) mice expressed high levels of intracellular Bim protein. Taken together, the increased apoptosis and elevated Bim levels observed in Drosha-, DGCR8-, and Dicer-deficient pre-B cells underscore the critical role of miRNAs in pre-B cell survival.

Our previous analysis of Dicer-deficient B cells had identified the tumor suppressor PTEN as being upregulated in these cells (Koralov et al., 2008). Accordingly, intracellular levels of PTEN were higher in DGCR8- and Drosha-deficient pro-B and pre-B cells compared to control cells (Figures 1D and S2C). PTEN is a negative regulator of the PI3K pathway known to play an important role in cell-cycle regulation (Sun et al., 1999) and B cell development (Werner et al., 2010). Large pre-B cells (FSC^{hi}B220^{+}CD25^{+}ckit^{-}IgM^{-}) are characterized by the rapid

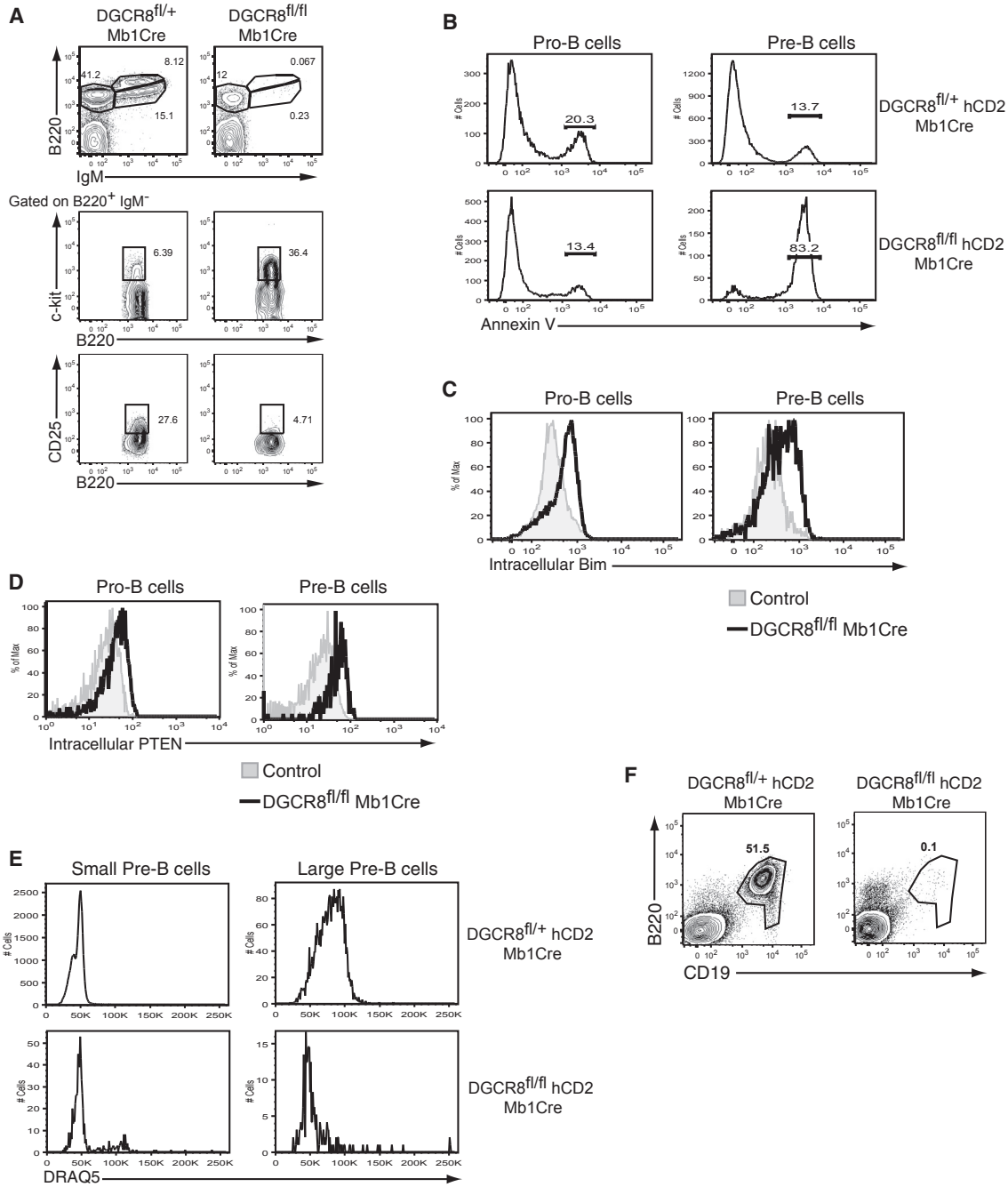

Figure 1. Block in Early B Cell Development in Absence of Microprocessor Complex

(A) Representative FACS plots of bone marrow from *Dgcr8*$^{fl/fl}$ *Mb1*-cre and *Dgcr8*$^{fl/+}$ *Mb1*-cre control animals. Events are gated on total lymphocytes. Plots showing pro-B cells (B220^{+}c-kit^{+}) and pre-B cells (B220^{+}CD25^{+}) cells are gated on B220^{+} IgM^{-} B lymphocyte progenitor cells (n > 5 mice).

(B) Representative Annexin V staining of pro-B and pre-B cells gated as in (A) from mice of the indicated genotypes (n > 5 mice).

(C and D) Representative histograms for intracellular Bim (C) and PTEN (D) staining on pro-B and pre-B cells gated as in (A) from *Dgcr8*$^{fl/fl}$ *Mb1*-cre (solid line) or control (shaded) mice (n > 5 mice).

(E) DNA content analysis assayed using DRAQ5 incorporation from small or large pre-B cells (gated on B220^{+}IgM^{-}CD25^{-} then gated on size) from BM of animals with B cell-specific deficiency in DGCR8 (n > 5 mice).

(F) Representative FACS analysis of spleen from *Dgcr8*$^{fl/fl}$ *mb1*-cre and control animals. Events are gated on total lymphocytes. (n ≥ 5 mice).

See also Figures S1 and S2.

proliferation that takes place prior to *IgL* chain recombination at the small pre-B cell stage. To examine the role of miRNAs in the regulation of cell-cycle progression during B cell development, we examined DNA content in small and large pre-B cells. We found that the fraction of large pre-B cells was severely reduced and that these cells appeared to be arrested in cell-cycle progression at the G0/G1 stage in the absence of Dicer, Drosha, or DGCR8, as determined by staining of the cells with the DNA intercalating dye DRAQ5 (Figures 1E and S2D). Taken together, our data suggest that the reduction of the pre-B cell compartment and the developmental B cell block observed in the absence of Dicer, Drosha, or DGCR8 could be attributed to both increased cell death and decreased proliferation, as a consequence of the lack of miRNAs.

Consistent with the severe developmental block in the bone marrow, we observed a paucity of splenic B cells in absence of DGCR8, Drosha, and Dicer. Spleens of *Dgcr8*$^{fl/fl}$ *Mb1*-cre and *Drosha*$^{fl/fl}$ *Mb1*-cre mice were largely devoid of B cells as shown by the drastic decrease in B220^{+} CD19^{+} B cell percentage and cell number compared to controls (Figures 1F, S1C, and S1D) similar to the lack of peripheral B cells that we have previously observed in *Dicer1*$^{fl/fl}$ *Mb1*-cre animals (Koralov et al., 2008).

A Bcl2 Transgene Is Capable of Partially Rescuing Drosha- and DGCR8-Deficient B Cells

To rescue B cell development in *Dgcr8*$^{fl/fl}$ *Mb1*-cre and *Drosha*$^{fl/fl}$ *Mb1*-cre mice, we took advantage of a Bcl2 transgene (Tg) restricted to the B cell lineage (EμBcl2^{Tg}) (Strasser et al., 1991), as we have previously demonstrated that Bcl2 overexpression partially rescues B cell development in the absence of Dicer (Koralov et al., 2008). While B cell development was still compromised, we observed a reduced accumulation of pro-B cells accompanied by a slight increase in pre-B cells in *Dgcr8*$^{fl/fl}$ *Mb1*-cre EμBcl2^{Tg} mice compared to the *Dgcr8*$^{fl/fl}$ *Mb1*-cre animals (Figures 2A and 2B). The percentage of immature and recirculating cells was significantly higher in *Dgcr8*$^{fl/fl}$ *Mb1*-cre EμBcl2^{Tg} mice compared to *Dgcr8*$^{fl/fl}$ *Mb1*-cre mice (Figure 2B). The developmental block was similarly attenuated by the expression of Bcl2 in Drosha-deficient mice (Figure 2C) as in Dicer-deficient mice (Koralov et al., 2008).

Despite the B cell intrinsic loss of miRNAs in the absence of either of the three enzymes required for RNAi, there was a distinct population (~12%) of B220^{+}CD19^{+} B cells in the spleens of *Dgcr8*$^{fl/fl}$ *Mb1*-cre EμBcl2^{Tg} and *Drosha*$^{fl/fl}$ *Mb1*-cre EμBcl2^{Tg} mice analogous to what we had previously observed in *Dicer1*$^{fl/fl}$ *Mb1*-cre EμBcl2^{Tg} mice (Figures 3A–3C and S3A). Thus, ectopic expression of the pro-survival EμBcl2^{Tg} resulted in partial rescue of B cell development and accumulation of peripheral B cells in the absence of either DGCR8, Drosha, or Dicer.

To evaluate whether B cells lacking DGCR8, Drosha, or Dicer and rescued with the EμBcl2^{Tg} exhibited an equal loss of mature miRNAs, we examined levels of members of the miR-17~92 family of miRNAs, previously shown to be important for B cell development (Koralov et al., 2005; Ventura et al., 2008), as well miR-142-5p and miR-181a, which are highly expressed in murine B cells (Chen et al., 2004; Landgraf et al., 2007). These miRNAs were decreased at least 10-fold in B220^{+} CD19^{+} B cells sorted from *Dgcr8*$^{fl/fl}$ *Mb1*-cre EμBcl2^{Tg} mice compared to control B cells (Figure 3D and data not shown). A similar decrease in miRNA expression was observed in B cells from *Drosha*$^{fl/fl}$ *Mb1*-cre EμBcl2^{Tg} mice (Figure S3B). The traces of miRNAs detected in knockout (KO) B cells by real-time PCR may either represent the remaining average levels of mature miRNAs in the sorted cells or may come from the few cells in the total B cell pool that have escaped *Mb1*-cre-mediated deletion of the targeted alleles.

Most Bcl2 Rescued miRNA-Deficient B Cells Display Low Surface Ig Expression

The partial rescue of RNAi-deficient B cells upon expression of transgenic Bcl2 allowed us to further explore the role of Dicer, Drosha, and DGCR8 in mature splenic B lymphocytes. Staining these cells for a variety of surface markers, we observed that up to ~75% of the rescued DGCR8 KO, Drosha KO, and Dicer KO B cells expressed levels of surface IgM that were markedly lower than the levels on control cells (Figures 4A, S4A and S4B). We designated the cells with low expression of surface IgM, "Ig^{low}" cells and cells expressing surface IgM levels similar to Bcl2 control cells, "Ig^{high}" cells. The Ig^{low} RNAi-deficient B lymphocytes otherwise expressed the typical B cell markers that we examined (including CD19, B220, CD23, and CD21) (data not shown). They did not appear to be plasma cells based on fluorescence-activated cell sorting (FACS) analysis and morphology (CD138 and FSC parameters were examined; data not shown). We then considered whether the Ig^{low} DGCR8 KO, Drosha KO, and Dicer KO B cells may have a defect in the processing of the μ heavy chain that requires alternative splicing between the c4 and m1 exons for expression of membrane-bound antibody (Alt et al., 1980; Early et al., 1980; Rogers et al., 1980). However, real-time PCR analysis of mRNA levels for the two alternative forms of the μ heavy chain revealed that Ig^{low} B cells from all three mutants showed a comparable (albeit lower) ratio of secreted to membrane splice variants compared to B cells from control mice (Figure S4C). This suggests that altered splicing of Igμ mRNA was not responsible for the Ig^{low} phenotype in the absence of RNAi.

In an effort to further characterize Ig^{low} B cells, we examined surface expression and intracellular protein level of Igμ heavy chains as well as Igκ and Igλ light chains in these cells. FACS analysis revealed that despite low surface levels of Igμ, most Ig^{low} cells stained positive for intracellular Igμ, with most cells having comparable levels to those observed in B cells from littermate controls (Figure 4B). Surface staining for Ig light chains revealed that Ig^{low} cells from *Dgcr8*$^{fl/fl}$ *Mb1*-cre EμBcl2^{Tg} animals lack any detectable surface expression of Igκ or Igλ, while Ig^{high} cells have an unusually high fraction of λ^{+} B cells (Figure 4C). The percentage of λ^{+} B cells was 2-fold higher in Bcl2 control mice compared to wild-type littermates (data not shown), consistent with previous observations (Lang et al., 1997), but the Ig^{high} miRNA-deficient B cell compartment contained as many as 10%–25% λ^{+} B cells. Intracellular analysis of Igκ and Igλ light chains demonstrated that indeed Ig^{low} cells were entirely devoid of detectable Ig light chain proteins (Figure 4D). These observations were recapitulated in B cells from *Drosha*$^{fl/fl}$ *Mb1*-cre EμBcl2^{Tg} and *Dicer1*$^{fl/fl}$ *Mb1*-cre EμBcl2^{Tg} mice (data not shown). Because Ig^{low} cells were expressing heavy chain without

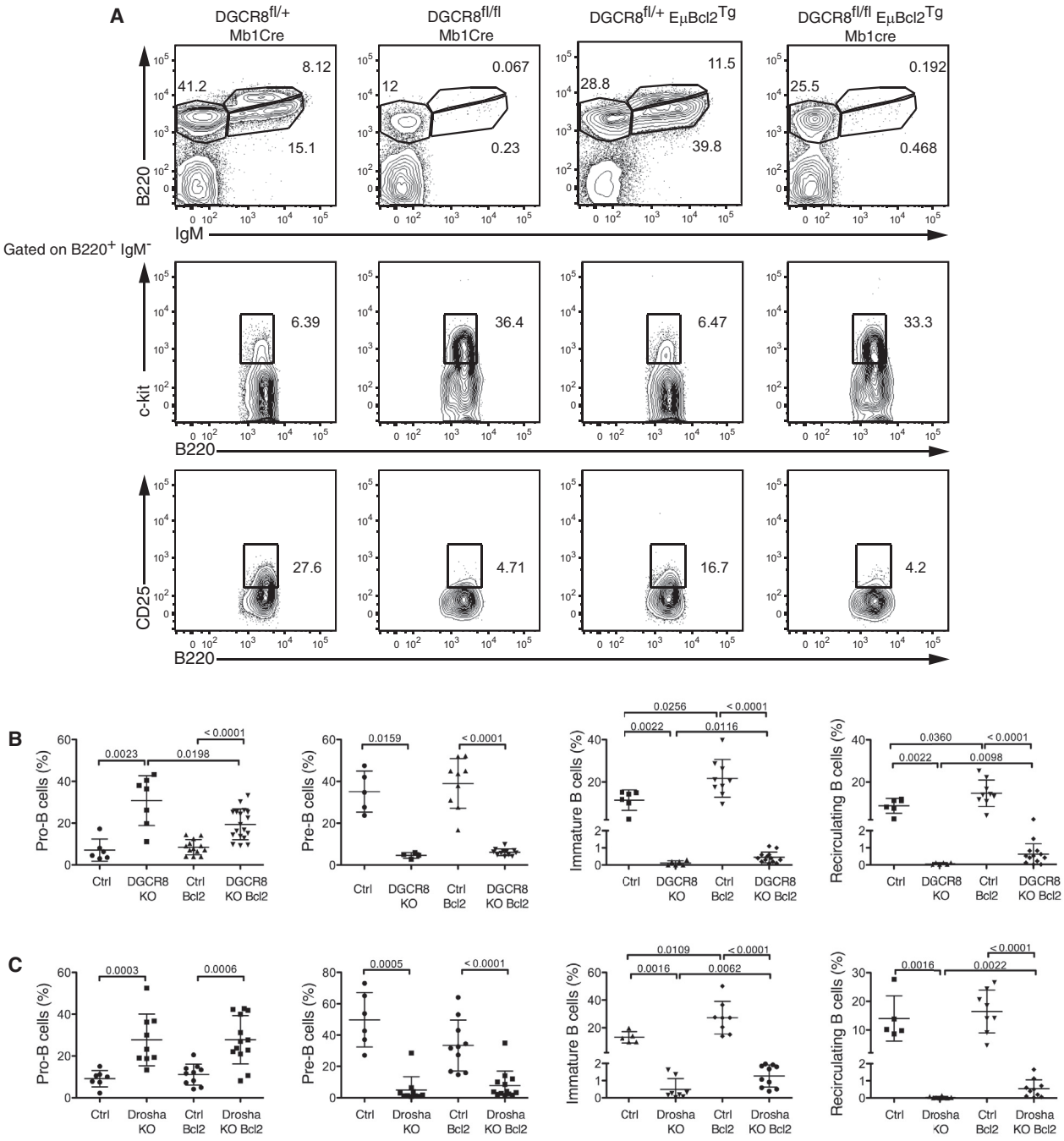

Figure 2. Partial Rescue of a Block in B Cell Development by Expression of a Bcl2 Transgene

(A) FACS analysis of bone marrow from *Dgcr8*$^{fl/fl}$ *Mb1*-cre, *Dgcr8*$^{fl/fl}$ *Mb1*-Cre EμBcl2^{Tg}, and control mice. The top panels are gated on total lymphocytes. The two bottom panels are gated on B220^{+}IgM^{-} progenitor cells ($n \geq 5$ in each group).

(B and C) Frequency of pro- and pre-B cells gated as in (A), plotted as a percentage of B220^{+}IgM^{-} progenitors in the BM. Frequency of immature (B220^{+}IgM^{+}) and recirculating (B220^{high}IgM^{+}) B cells plotted as percentage of lymphocytes in the BM. DGCR8 KO (*Dgcr8*$^{fl/fl}$ *Mb1*-cre), DGCR8 KO Bcl2 (*Dgcr8*$^{fl/fl}$ *Mb1*-cre EμBcl2^{Tg}), Drosha KO (*Drosha*$^{fl/fl}$ *Mb1*-Cre), and Drosha KO Bcl2 (*Drosha*$^{fl/fl}$ *Mb1*-Cre EμBcl2^{Tg}). Ctrl and Ctrl Bcl2 indicate the appropriate control mice without and with Bcl2, respectively. Each dot is representative of one mouse, $n \geq 5$ in each group (central horizontal bar indicates the mean with SD). P value is indicated when <0.05.

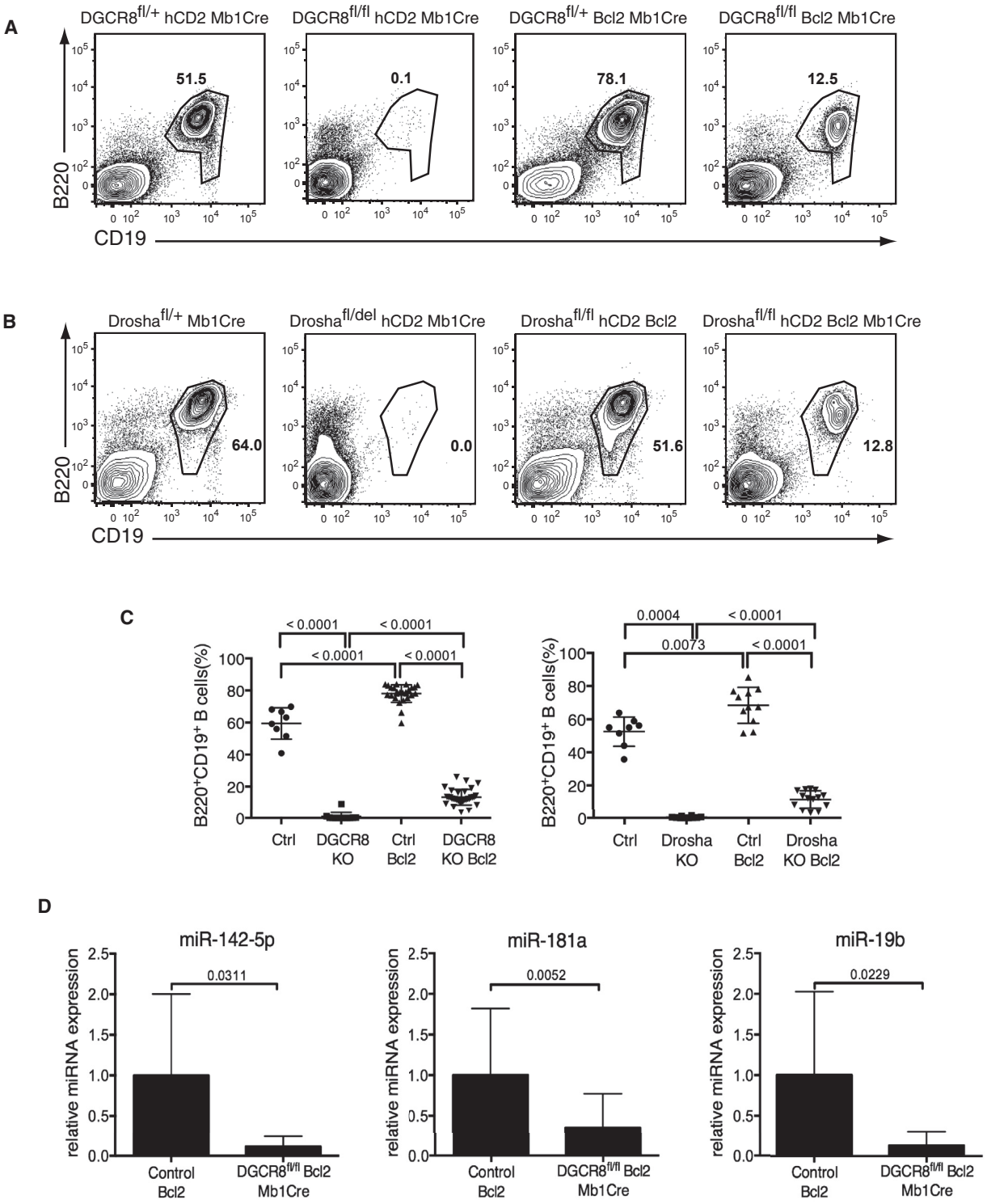

Figure 3. Bcl2 Transgene Mediates Partial Rescue of RNAi-Deficient B Cells

(A and B) Representative FACS analysis of B220 and CD19 straining on spleen of the indicated mice ($n \geq 7$ mice per group).

(C) Percentage of $B220^{+}CD19^{+}$ B cells in the spleen of the indicated mice labeled as in Figure 2B. (mean ± SD). P values <0.05 are indicated.

(D) Loss of miRNAs in *Dgcr8*$^{fl/fl}$ *Mb1*-cre EμBcl2^{Tg} mice is shown by real-time PCR of a representative set of miRNAs on sorted B cells from the indicated mice. Data is normalized against U6 and represented relative to the control cells, $n \geq 7$ for both groups (mean ± SD).

See also Figure S3.

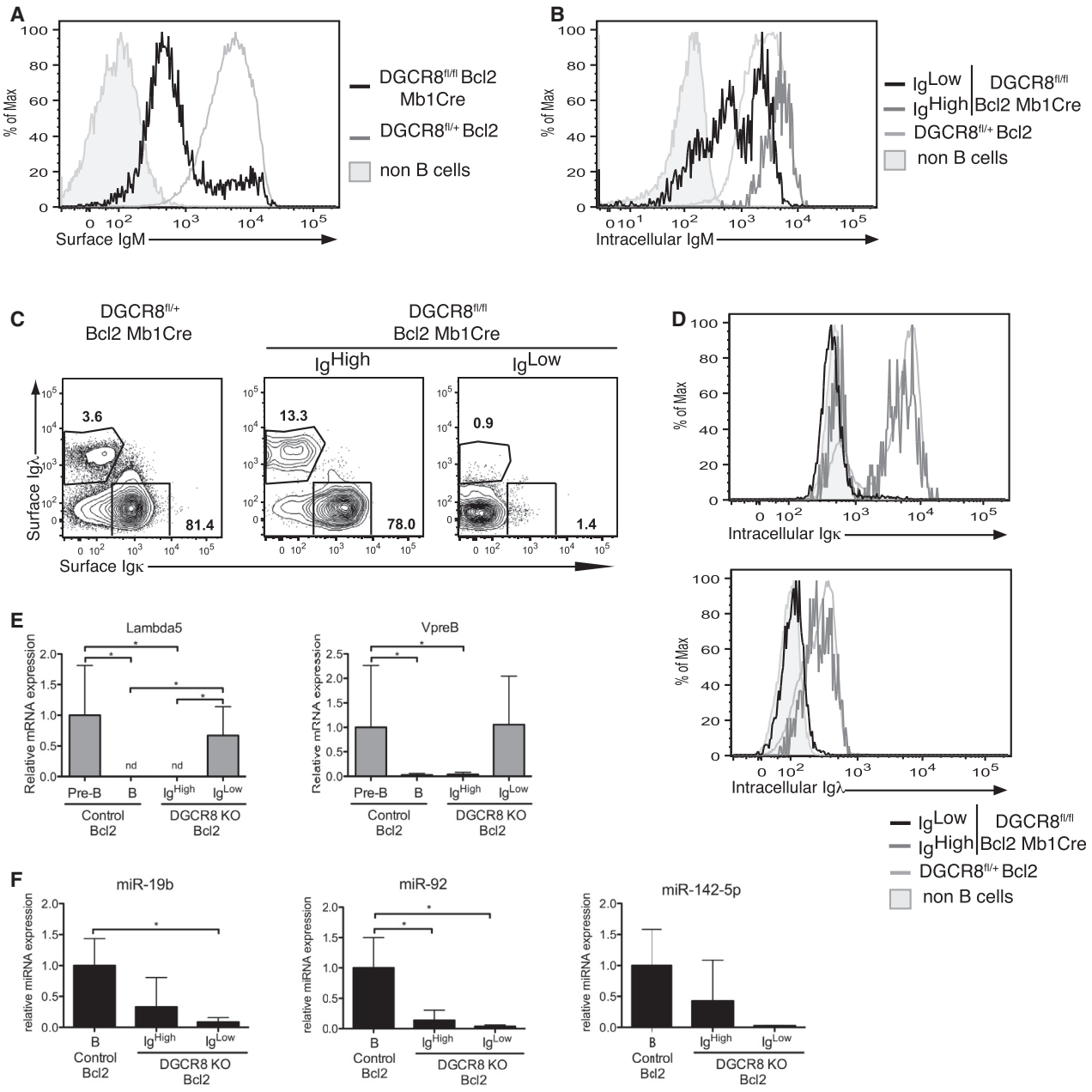

Figure 4. Majority of RNAi-Deficient B Cells Fail to Express Normal Surface Ig Levels

(A) Surface IgM levels of B220^{+}CD19^{+} B cells from the spleen of *Dgcr8*$^{fl/fl}$ *Mb1*-cre EμBcl2^{Tg} (black histogram) and *Dgcr8*$^{fl/+}$ EμBcl2^{Tg} mice (gray histogram). Non-B (B220^{-}CD19^{-}) lymphocytes were used as a staining control (shaded histogram) (n > 15).

(B) Intracellular IgM levels of B220^{+}CD19^{+} B cells of *Dgcr8*$^{fl/+}$ EμBcl2^{Tg} mice (light gray histogram) or of Ig^{high} (dark gray) or Ig^{low} (black) cells (as gated on surface Igμ levels) from *Dgcr8*$^{fl/fl}$ *Mb1*-cre EμBcl2^{Tg} as well as non-B lymphocytes (shaded histogram). Data is representative of >15 independent experiments.

(C) Representative FACS analysis of Igκ and Igλ on the surface of B220^{+}CD19^{+} splenic B cells of *Dgcr8*$^{fl/+}$ *Mb1*-cre EμBcl2^{Tg} mice and on the Ig^{high} or Ig^{low} cells (gated based on surface Igμ levels) from the same *Dgcr8*$^{fl/fl}$ *Mb1*-cre EμBcl2^{Tg} animals (n > 15).

(D) Intracellular staining for Igκ (top) or Igλ (bottom) in B220^{+}CD19^{+} splenic B cells as in (B) (n > 15).

(E) Expression of the surrogate light chain component λ5 and VpreB mRNA was determined by real-time PCR in Ig^{high} and Ig^{low} B220^{+}CD19^{+}CD25^{-} B cells sorted according to surface IgM expression from spleens of *dgcr8*$^{fl/fl}$ *Mb1*-cre EμBcl2^{Tg} (DGCR8 KO Bcl2) or *Mb1*-cre EμBcl2^{Tg} expressing control mice. Data normalized to *hprt* are relative to pre-B cells from control bone marrow (mean ± SD indicated; more than three independent experiments. *p % 0.05).

(F) miRNAs levels were assayed by real-time PCR in Ig^{high} or Ig^{low} B220^{+}CD19^{+}CD25^{-} B cells sorted based on surface IgM expression from spleen of mice deficient or not for DGCR8 and expressing EμBcl2^{Tg}. Data is normalized to U6 and represented relative to control cells (mean ± SD indicated; more than three independent experiments. *p ≤ 0.05).

See also Figure S4.

light chain at their surface, we hypothesized that Igμ may be co-expressed with the pre-BCR components λ5 and VpreB. Analysis of gene expression by real-time PCR revealed that the genes encoding these proteins, whose expression is normally limited to the progenitor B cells in the bone marrow, were expressed in Ig^{low} but not Ig^{high} B cells from *Dgcr8*$^{fl/fl}$ *Mb1*-cre EμBcl2^{Tg}, *Drosha*$^{fl/fl}$ *Mb1*-cre EμBcl2^{Tg}, and *Dicer1*$^{fl/fl}$ *Mb1*-cre EμBcl2^{Tg} mice (Figure 4E and data not shown). As expected, B cells from control animals did not have any detectable expression of the pre-BCR components.

The presence of two seemingly distinct populations of B cells, Ig^{high} and Ig^{low}, among the Bcl2 Tg-rescued miRNA-deficient B cells raised the question of how complete the deletion of Dicer, Drosha, or DGCR8 was in these lymphocytes. We sorted Ig^{low} and Ig^{high} cells from *Dgcr8*$^{fl/fl}$ *Mb1*-cre EμBcl2^{Tg}, *Drosha*$^{fl/fl}$ *Mb1*-cre EμBcl2^{Tg}, and *Dicer1*$^{fl/fl}$ *Mb1*-cre EμBcl2^{Tg} mice as well as cells from control animals and performed real-time PCR analysis of *Dgcr8*, *Drosha*, and *Dicer* mRNA. *Drosha*, *Dgcr8*, or *Dicer* transcripts were barely detectable in both Ig^{low} and Ig^{high} cells from the corresponding mice (Figure S4D). In addition, cells from *Dgcr8*$^{fl/fl}$ *mb1*-cre EμBcl2^{Tg} mice, irrespective of whether Ig^{low} or Ig^{high}, expressed low levels of, if any, miRNAs. The average levels of miRNAs that we examined did appear higher in Ig^{high} compared to Ig^{low} cells, consistent with the possibility that the Ig^{high} cells represented precursors of Ig^{low} lymphocytes (Figure 4F). Similar results were obtained for cells purified from *dicer1*$^{fl/fl}$ *Mb1*-cre EμBcl2^{Tg} and *Drosha*$^{fl/fl}$ *Mb1*-cre EμBcl2^{Tg} mice (data not shown).

Light Chain Editing in Peripheral Rescued B Cells Lacking miRNAs

We sorted Ig^{high} and Ig^{low} B cells from the spleens of *Dgcr8*$^{fl/fl}$ *Mb1*-cre EμBcl2^{Tg} mice as well as B cells from control mice expressing EμBcl2^{Tg} and investigated whether the absence of Ig light chains in Ig^{low} cells was due to impaired *Ig* light chain gene rearrangement. These rearrangements generally start at the *Igκ* locus with Jκ1 and Jκ2 preferentially rearranged (Nishi et al., 1985; Vela et al., 2008). Sequencing of the Vκ-Jκ joints in Ig^{low} cells revealed skewing toward the more distal Jκ4 and Jκ5 usage in *Igκ* joints (Figure S5A) and predominantly non-productive out-of-frame joints (Figure S5B) suggesting secondary light chain rearrangements in these cells. Analysis of the different cell populations by real-time PCR of genomic DNA revealed increased levels of rearrangement between a Vκ gene element and the recombining sequence (RS) or between the intronic RS (IRS) and RS in splenic B cells from *Dgcr8*$^{fl/fl}$ *Mb1*-cre EμBcl2^{Tg} Ig^{low} cells (Figure 5A). Recombinations involving RS remove or invert the κ light chain constant region, inactivating expression of the *Igκ* allele and allowing recombination to occur on the second *Igκ* allele or alternatively on one of the *Igλ* alleles (Vela et al., 2008). We found that Ig^{low} cells, and to a lesser extent Ig^{high} cells, had increased Vλ-Jλ1 rearrangements compared to control cells (Figure 5A). These findings suggested that there was increased light chain editing occurring in *Dgcr8*$^{fl/fl}$ *Mb1*-cre EμBcl2^{Tg} B cells as well as in *Dicer1*$^{fl/fl}$ *Mb1*-cre EμBcl2^{Tg} and *Drosha*$^{fl/fl}$ *Mb1*-cre EμBcl2^{Tg} B cells (Figure S5C and data not shown). Light chain editing is known to occur either in pre-B cells that fail to acquire an in-frame/functional rearrangement on one of the *Ig* light chain loci, or in pre-B cells that acquire a self-reactive BCR. We examined the *Igκ* locus in *Dgcr8*$^{fl/fl}$ *Mb1*-cre EμBcl2^{Tg} pre-B cells to investigate if editing in the absence of DGCR8 was occurring at the pre-B cell stage. We found that in the RNAi-deficient pre-B cells the Igκ locus was in the germline configuration at least as often as in control pre-B cells (i.e., did not show evidence of ongoing rearrangement). Furthermore, DGCR8-deficient pre-B cells had similar levels of Vκ-RS recombination and Vλ-Jλ1 rearrangement to control pre-B cells (Figure 5B). These data suggested that secondary light chain rearrangement was not occurring at higher levels in KO pre-B cells within the BM compared to control pre-B cells, but rather that the increase in editing that we observed in Ig^{low} cells occurred after the developing B cells left the BM compartment.

We studied colocalization of γH2AX, the phosphorylated form of H2AX, as a marker for DNA double-stranded breaks, with the *Igκ* loci by immuno-DNA fluorescence in situ hybridization (FISH) in splenic *Dicer1*$^{fl/fl}$ *Mb1*-cre EμBcl2^{Tg} Ig^{low} cells. We used two probes that hybridize 5′ and 3′ of the *Igκ* locus respectively together with an antibody against γH2AX. We found that the percentage of cells with γH2AX colocalized with *Igκ* was significantly higher in Ig^{low} cells compared to control or Ig^{high} cells, suggesting that *Igκ* rearrangement was occurring in Ig^{low} cells more frequently than in the other two populations. The levels of γH2AX at the *Igκ* locus of Ig^{low} cells was only ∼2-fold lower than that observed in pre-B cells from control mice (Figures 5C and 5D; Table S1). Taken together, our data suggest that light chain editing is ongoing in Ig^{low} splenic miRNA-deficient B cells.

Increased *Rag* and FOXO1 Expression in miRNA-Deficient Splenic B Cells

Ig gene recombination and editing is mediated by RAG1 and RAG2, both normally expressed in pro-B and pre-B cells, with no detectable transcription in peripheral B cells (Han et al., 1997; Hikida et al., 1996). However, in RNAi-deficient Ig^{low} B cells, *Rag1* and *Rag2* mRNA was readily detectable, consistent with ongoing *Ig* light chain rearrangement. Expression of these genes in Ig^{low} cells, albeit at significantly lower levels compared to pre-B cells, suggests that *Ig* light chain rearrangement in Ig^{low} cells is mediated by expression of RAG1 and RAG2. As expected, control splenic B cells did not express detectable levels of either *Rag1* or *Rag2*. *Rag1* and *Rag2* transcripts were also undetectable in the RNA from *Dgcr8*$^{fl/fl}$ *Mb1*-cre EμBcl2^{Tg} Ig^{high} cells (Figure 6A)

While Ig^{low} cells lack expression of progenitor markers such as c-kit, CD43, and CD25, we wanted to exclude the possibility that the observed expression of *Rag1/2* in these cells was due to contaminating pre-B cells. For this purpose, we treated *Dgcr8*$^{fl/fl}$ *Mb1*-cre EμBcl2^{Tg} and EμBcl2^{Tg} control mice with anti-IL7Rα antibody for 2 weeks (Figure S6A) to arrest B cell development and thus prevent bone marrow output of pre-B cells (Sudo et al., 1993). Ig^{low} cells sorted from the treated animals expressed both *Rag1* and *Rag2* at levels similar to non-treated mice (Figure S6B). These results demonstrate that RNAi-deficient Ig^{low} cells are not bone marrow-derived progenitor cells. Furthermore, the data also suggest that expression of *Rag1/2* in the Ig^{low} B cells is independent of IL-7. To further validate these results, we used an independent approach where we

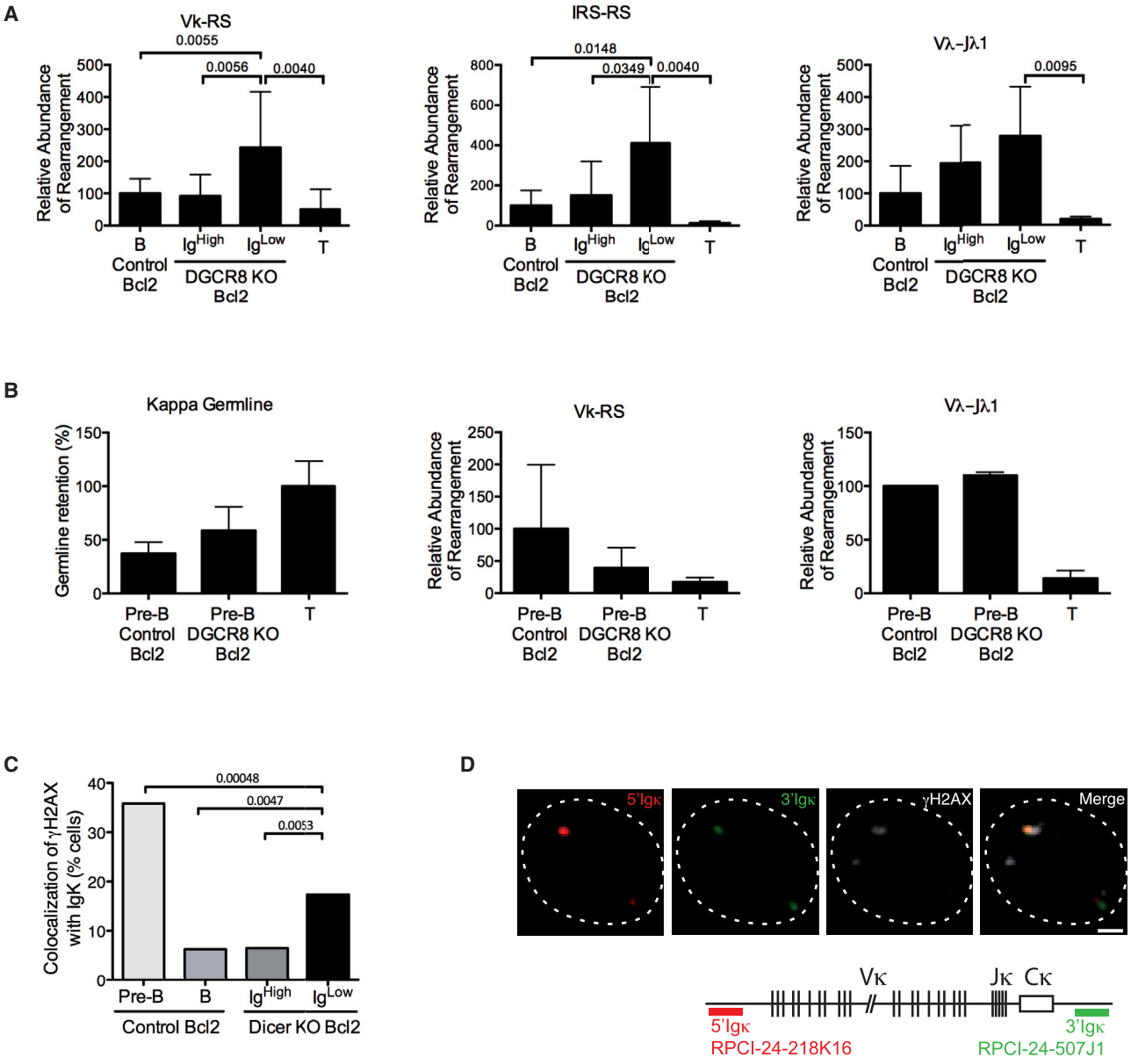

Figure 5. Ongoing Light Chain Editing in Ig^{low} Cells

(A) Light chain rearrangement was assessed by real-time PCR of Vκ-RS, IRS-RS, and Vλ-Jλ1 joints in the gDNA from DGCR8-deficient (DCGR8 KO Bcl2) or sufficient (control Bcl2) splenic B220^{+}CD19^{+}CD25^{-} B cells sorted according to surface IgM levels into Ig^{high} and Ig^{low} cells. Data is normalized to λ5 and levels in control cells set as 100%. T cells from control mice are used as a negative control. Values shown are mean ± SD of more than three independent experiments.

(B) Germline status of the κ alleles and ongoing light chain rearrangement at the *IgL* loci was evaluated in control or DGCR8-deficient pre-B cells sorted from the bone marrow of *Dgcr8*$^{fl/fl}$ *Mb1*-cre EμBcl2^{Tg} (DGCR8 KO Bcl2) and *Dgcr8*$^{fl/+}$ *Mb1*-cre EμBcl2^{Tg} (control Bcl2) animals. Data is normalized to λ5 and plotted relative to control EμBcl2^{Tg} pre-B cells. Values shown are mean ± SD of more than three independent experiments.

(C) Immuno-DNA FISH of the frequency of γH2AX association with *Igk* loci in control EμBcl2^{+} pre-B, control B or Ig^{high}, and Ig^{low} B220^{+}CD19^{+}CD25^{-} B cells sorted according to surface IgM expression from spleens of *Dicer1*$^{fl/fl}$ *Mb1*-cre EμBcl2^{Tg} (Dicer KO Bcl2) cells. Data are displayed as a combination of two independent experimental sets ($n \geq 133$ cells for each genotype; see Table S1 for individual datasets).

(D) Top: confocal microscopy sections of two *Igk* loci with a γH2AX focus on one locus. 5′*Igk* in green, 3′*Igk* in red, and γH2AX in white. Scale bar, 1 μm. Bottom: schematic of the positions of probes.

See also Figure S5.

induced in vivo deletion of Dicer in B cells by injecting three times poly(I:C) into *Dicer*$^{fl/fl}$ mice (Murchison et al., 2005) carrying the type 1 interferon-inducible *Mx1-cre* Tg (Kühn et al., 1995). One week after the last injection, B cell development in the bone-marrow was abrogated, and there were virtually no transitional (AA4.1^{+} B220^{+}) B cells in the spleen (Figure S6C). We found

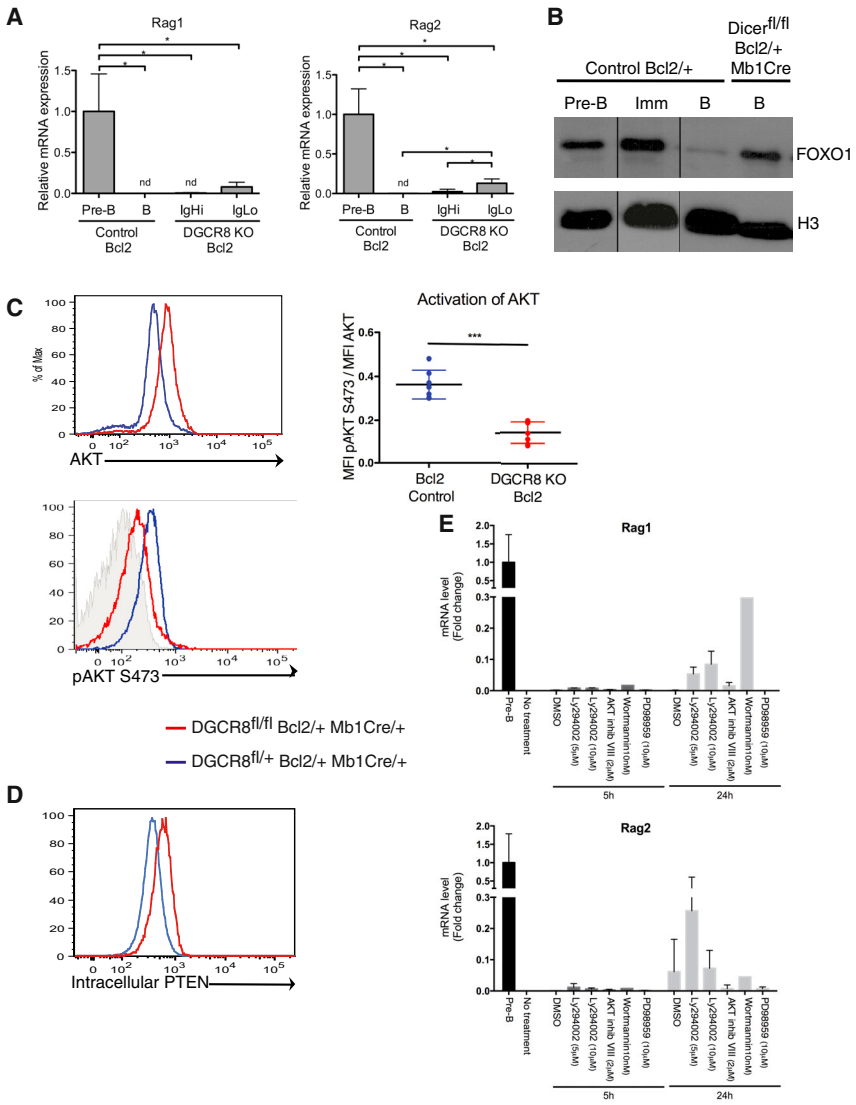

Figure 6. Downregulation of AKT Activity Leads to Increase FOXO1 and *Rag1/2* Levels in RNAi-Deficient B Cells

(A) Transcript levels of *Rag1* and *Rag2* in $B220^{+}CD19^{+}CD25^{-}$ Ig^{high} or Ig^{low} splenic B cells deficient for DGCR8 (DGCR8 KO Bcl2) or in control B cells expressing Bcl2 Tg (Control Bcl2). Data is normalized to *hprt* and represented as relative to $E\mu Bcl2^{Tg}$ control pre-B cells. Values shown are mean ± SD of more than three independent experiments. *$p \leq 0.05$.

(B) Western blot analysis of FOXO1 in purified splenic $B220^{+}CD19^{+}CD25^{-}$ B cells from *Dicer1*$^{fl/fl}$ *Mb1*-cre $E\mu Bcl2^{Tg}$ or *control* $E\mu Bcl2^{Tg}$ mice. Histone H3 was used as a loading control. The black vertical lines indicate that unrelated samples were run on the same gel in between the different samples shown.

(C) Intracellular levels of total AKT (top) and phospho-AKT (Ser473) (bottom) in $B220^{+}$ B cells from the spleen of *Dgcr8*$^{fl/fl}$ *Mb1*-cre $E\mu Bcl2^{Tg}$ (red line) or control (blue line) mice. Background levels are shown by the shaded histogram. AKT activation as defined by the ratio of the median fluorescence intensity (MFI) of pAKT to total AKT MFI (mean ± SD; n = 6 mice, ***p value < 0.001).

(D) Histogram of intracellular PTEN in $B220^{+}CD19^{+}$ B cells from the spleen of *Dgcr8*$^{fl/fl}$ *Mb1*-cre $E\mu Bcl2^{Tg}$ (red line) or control (blue line) mice (n > 6 mice).

(E) Transcript levels of *Rag1* and *Rag2* in wild-type mature ($B220^{+}CD19^{+}AA4.1^{-}$) B cells cultured for the indicated time with the PI3K inhibitors (Ly294002 and Wortmannin), the AKT inhibitor (AKT inhibitor VIII), the ERK inhibitor (PD98959) or DMSO. Data is normalized to *hprt* and represented relative to $E\mu Bcl2^{Tg}$ control pre-B cells. Values shown are mean ± SD of three independent experiments.

See also Figure S6.

that B cells from the spleen of Dicer ablated mice expressed readily detectable levels of *Rag1/2* mRNA (Figure S6D).

Rag1 and *Rag2* were expressed in Dicer- Drosha-, and DGCR8-deficient EμBcl2 rescued Ig^{low} cells suggesting that miRNAs regulate *Rag1* and *Rag2* mRNA expression. Transcription of *Rag1* and *Rag2* during light chain rearrangement and receptor editing in pre-B and immature B cells have been shown to be regulated by forkhead box O (FOXO)1 downstream of the PI3K/AKT pathway (Amin and Schlissel, 2008; Herzog et al., 2008). We investigated if this pathway was also involved in the BCR editing observed in miRNA-deficient Ig^{low} cells. While FOXO1 protein is expressed at very low levels in control splenic B cells, it was readily detectable in pre-B and bone marrow immature B cells sorted from control animals, consistent with the ongoing light chain *Ig* rearrangement in these cells. Levels of total FOXO1 were highly elevated in sorted splenic B cells from *Dicer*$^{fl/fl}$ *Mb1*-cre $E\mu Bcl2^{Tg}$ mice as determined by western blot analysis (Figure 6B). Levels of *Foxo1* mRNAs were similar in DGCR8-deficient or proficient B cells suggesting a post-transcriptional regulation of *Foxo1* (Figure S6E). Cellular localization and levels of FOXO1 protein are regulated by AKT-mediated FOXO1 phosphorylation. Phosphorylated FOXO1 is exported from the nucleus into the cytoplasm where it is degraded (Tzivion et al., 2011). We found increased FOXO1 levels in miRNA-deficient B cells suggesting that phosphorylation of FOXO1 and subsequent degradation is compromised in absence of miRNAs. Intracellular staining revealed increased levels of total AKT in splenic B cells of *Dgcr8*$^{fl/fl}$ *Mb1*-cre $E\mu Bcl2^{Tg}$ and *Dicer1*$^{fl/fl}$ *Mb1*-cre $E\mu Bcl2^{Tg}$ mice when compared to AKT levels from control B cells (Figures 6C, top, and data not shown). AKT activation is dependent on its phosphorylation at Th308 and S437 residues (Sarbassov et al., 2005; Stephens et al., 1998). A strong decrease in S473 phosphorylation of AKT was observed in RNAi-deficient B cells (Figure 6C, bottom). We used the ratio of median fluorescence intensity (MFI) of phosphorylated AKT to the MFI of total AKT to assess the activation of the AKT

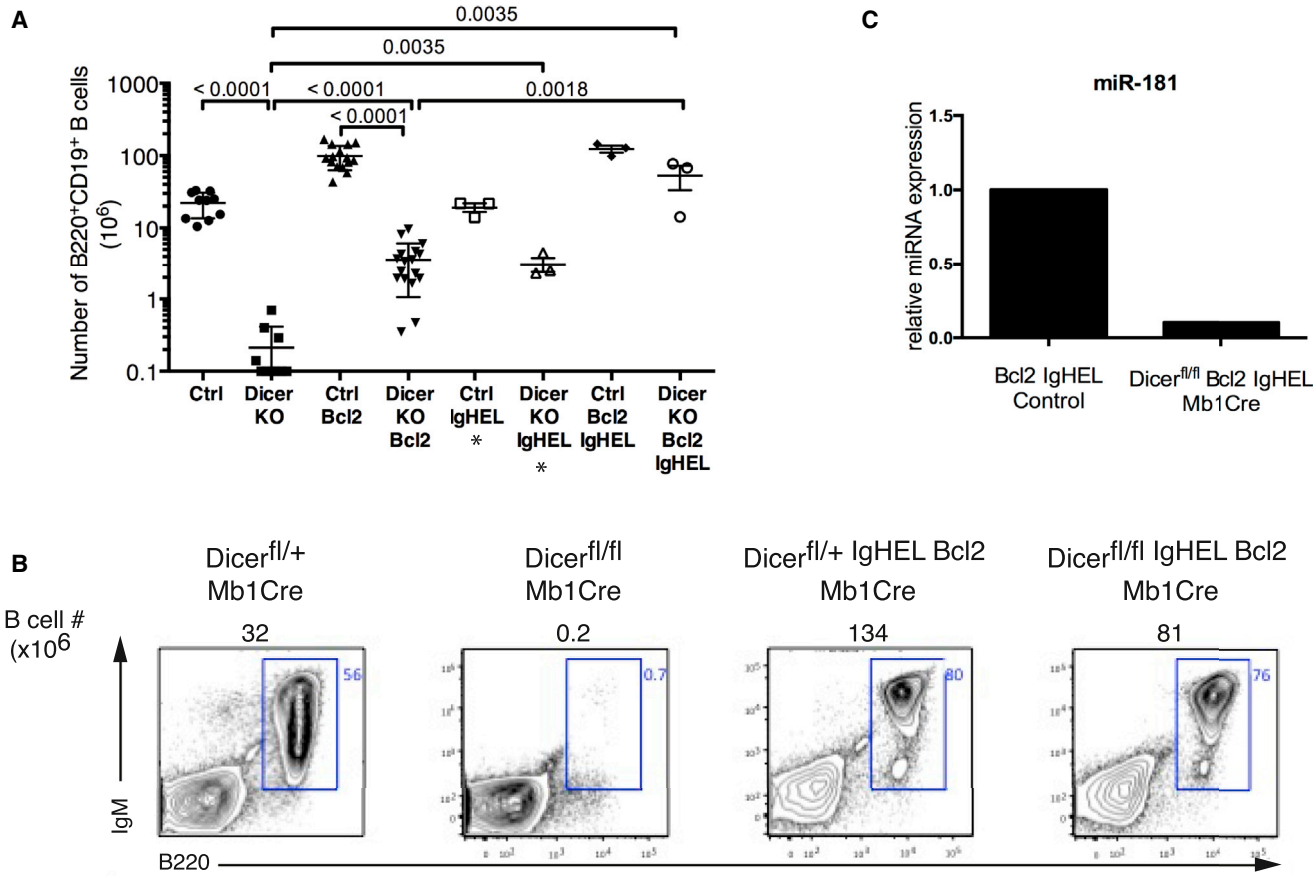

Figure 7. Complete B Cell Rescue with EμBcl2 and IgHEL Transgene in Absence of Dicer

(A) Number of B220^{+}CD19^{+} B cells in the spleen of the indicated mice. Data from the mice expressing IgHEL by itself and marked with an asterisk has been previously described (Koralov et al., 2008) (mean ± SD, n ≥ 3, p values are shown when significant).

(B) Representative FACS plots of B220 and IgM staining in the spleen of mice of the indicated genotype. Number in graph indicates percentage of cells in the gate. Number above graph indicates the B cell number in the spleen of the indicated mice (n ≥ 3).

(C) Levels of miR-181 in *Dicer*$^{fl/fl}$ *Mb1*-cre EμBcl2^{Tg} IgHEL^{Tg} and control splenic B cells as determined by real-time PCR. Data is normalized to U6 and represented relative to control cells.

pathway. DGCR8-deficient and Dicer-deficient B cells had a significant decrease in AKT activation (Figure 6C, right, and data not shown) consistent with the increased levels of FOXO1 observed in these cells. pTh308 levels were also decreased in B cells lacking miRNAs (Figure S6F). Phosphorylation of AKT is downstream of PI3K activation and can be antagonized by PTEN. Consistent with previous reports that PTEN is directly regulated by several B cell intrinsic miRNAs (Benhamou et al., 2016; Gonzalez-Martin et al., 2016; Lai et al., 2016; Xiao et al., 2008) we found that PTEN levels were strongly elevated in miRNA-deficient B cells compared to B lymphocytes from control animals (Figure 6D).

We sorted wild-type splenic mature B cells (CD19^{+}B220^{+} AA4.1^{-}) and treated them in vitro with the PI3K inhibitors Ly294002 and Wortmannin as well as an AKT-specific inhibitor, AKT inhibitor VIII. Inhibition of PI3K in these mature B cells resulted in induction of *Rag1* and *Rag2* expression after 5 hr incubation and became more notable at 24 hr. Incubation with the AKT inhibitor also led to *Rag1* and *Rag2* expression, albeit to a lesser extent. Cells treated with DMSO as a vehicle control or an ERK inhibitor (PD98959), as well as non-treated mature B cells did not express *Rag1/2* (Figure 6E). These results suggest that the PI3K/AKT pathway regulates *Rag1/2* expression in mature B cells. Taken together, our findings demonstrate that miRNAs regulate *Rag1/2* expression through control of PTEN, AKT, and FOXO1 in mature B cells. Thus Dicer-, Drosha-, and DGCR8-dependent miRNAs are essential for the downregulation of BCR editing in peripheral B lymphocytes.

Complete Rescue of B Cell Development in the Absence of miRNAs by combined Expression of Bcl2 and IgHEL Transgenes

Bcl2-mediated rescue of B cell development in the absence of Dicer, Drosha, or DGCR8 was only partial (Figures 3 and 7A). We reasoned that expressing a EμBcl2 Tg together with a transgene for a functional BCR that cannot be edited would lead to a more complete rescue of miRNA-deficient B cells. We took advantage of a Tg encoding a fully rearranged BCR specific for hen egg lysozyme (HEL) (Goodnow et al., 1988). In the absence

of the pro-survival Bcl2 Tg, introduction of the IgHEL Tg by itself is sufficient to mediate only partial rescue of B cell development (~5%–10% of littermate controls) upon ablation of RNAi (Figure 7A). In contrast to the limited rescue of B cell development observed upon introduction of the individual transgenes (IgHEL or Bcl2), we observed that *Dicer1*$^{fl/fl}$ *Mb1*-cre EμBcl2^{Tg} IgHEL^{Tg} mice had a B cell compartment comparable in size to wild-type animals (Figures 7A and 7B). These rescued B cells had surface Ig levels comparable to *Mb1*-cre EμBcl2^{Tg}IgHEL^{Tg} control B lymphocytes (Figure 7B), but were indeed deficient in miRNAs (Figure 7C).

DISCUSSION

Our analysis of B lymphocytes deficient in the enzymes necessary for miRNA biogenesis revealed a critical role of miRNAs in the coordination of early B cell development and specifically in the maintenance of cell survival, proliferation, and regulation of Ig editing. By comparing Dicer-, Drosha-, and DGCR8-deficient B cells, we are able to confidently conclude that the observed phenotypes are a consequence of miRNA loss and are not due to loss of other classes of ncRNAs. We found that global loss of miRNAs early in B cell development resulted in a block at the pro-B to pre-B cell transition. This developmental defect was due to increased apoptosis of pre-B cells associated with high levels of the pro-apoptotic BH3 family member Bim in the deleted cells. Moreover, upregulation of PTEN in the absence of miRNAs led to reduced proliferation at the large pre-B cell stage. Our previous analysis of Dicer-deleted B cells identified the miR-17~92 family as a promising candidate for the regulation of both Bim and PTEN in developing B cells (Koralov et al., 2008). In addition, the analysis of mice deficient in miR-17~92 revealed a similar reduction in pre-B cells numbers, increased apoptosis of pro-B cells, and increased Bim levels in pro-B and pre-B cells (Ventura et al., 2008). miR-148, which is highly expressed in pro-B and pre-B cells, has recently been shown to target both Bim and PTEN in immature B cells (Gonzalez-Martin et al., 2016) and might also regulate their expression in early developing B cells. Our data suggest that miRNAs likely contribute to the regulation of pre-B cell proliferation and survival through the regulation of PI3K signaling via PTEN. These results are consistent with data, suggesting that signaling through the PI3K pathway, in particular downstream of the pre-BCR, is important for early B cell development especially for the survival and differentiation of pre-B cells (Werner et al., 2010). Furthermore, increased PTEN expression in the absence of miRNAs may also contribute to the elevated level of the pro-apoptotic protein Bim (Miletic et al., 2010).

As a result of the B cell developmental block, spleens of *Dicer1*$^{fl/fl}$ *Mb1*-cre, *Dgcr8*$^{fl/fl}$ *Mb1*-cre, and *Drosha*$^{fl/fl}$ *Mb1*-cre mice were almost completely devoid of B cells. Overexpression of the anti-apoptotic factor Bcl2 led to a partial rescue of B cells in the spleen of *Dicer1*$^{fl/fl}$ *Mb1*-cre *EμBcl2*^{Tg}, *Dgcr8*$^{fl/fl}$ *Mb1*-cre *EμBcl2*^{Tg}, and *Drosha*$^{fl/fl}$ *Mb1*-cre *EμBcl2*^{Tg} mice. The majority of the rescued B cells expressed lower levels of surface IgM than control *Mb1-cre EμBcl2*^{Tg} expressing B cells. These Ig^{low} cells lacked any detectable surface or intracellular Ig light chain and instead re-expressed λ*5* and *VpreB*. Ig^{low} cells had evidence of increased light chain editing as determined by real-time PCR and immuno-FISH experiments highlighting that the double strand breaks at the *Igκ* loci were occurring in the splenic Ig^{low} B cells. In addition, expression of the recombinase genes *rag*1/2 was readily detectable in splenic Ig^{low} cells even in mice where bone marrow output was halted by administration of an anti-IL-7Ra antibody. Furthermore, we could also detect expression of *Rag1* and *Rag2* mRNA in mature B cells upon ablation of Dicer from the spleen of *Dicer*$^{fl/fl}$ *Mx1Cre* mice by poly(I:C) injection. Taken together with the presence of DSBs at *Igκ* loci in Ig^{low} cells, the readily detectable expression of *Rag1* and *Rag2* indicated ongoing *IgL* gene rearrangement in peripheral B lymphocytes in the absence of miRNAs. Light chain editing can be associated with production or prevention of autoantibodies, however, when we assayed humoral responses using a highly sensitive validated multiplex assay, DGCR8-deficient adult mice were devoid of detectable IgG autoantibodies to a range of DNA/RNA-related autoantigens, while total serum IgG levels were <15% of control mice ($p < 0.008$, Mann Whitney, two-tailed) (not shown).

Our data suggest that miRNAs are potent regulators of *Rag1* and *Rag2*. The 3′UTR of the *Rag1* and *Rag2* mRNAs harbors very few putative target sites for miRNAs, and the few predicted sites that are revealed by Targetscan and PicTar algorithms are complementary to miRNAs that are not thought to be expressed in B lymphocytes. For this reason, *Rag1* and *Rag2* mRNAs are not likely to be direct targets of miRNAs. The PI3K pathway and the FOXO proteins, in particular FOXO1, have been shown to regulate expression of *Rag1* and *Rag2* during light chain rearrangement in pre-B cells and light chain editing in immature B cells lacking a functional light chain, expressing an auto-reactive BCR or having insufficient BCR "tonic" signal (Amin and Schlissel, 2008; Dengler et al., 2008; Diamant et al., 2005; Herzog et al., 2008; Verkoczy et al., 2007). Lymphocytes undergoing rearrangement display dampened PI3K/AKT signaling, promoting elevated nuclear levels of FOXO. We found that B cells lacking miRNAs had increased levels of the PI3K pathway antagonist PTEN. Consistently, phosphorylated and thus activated AKT levels were decreased in miRNA-deficient B cells even as total AKT levels were higher. This was associated with elevated levels of FOXO1 protein in miRNA-deficient B cells. In addition to its role in light chain rearrangement during B cell development, the PI3K/AKT/FOXO pathway has been shown to be important at later stages of B cell development—in particular in the regulation of AID in activated B lymphocytes (Dengler et al., 2008), the control of germinal center B cells (Sander et al., 2015; Dominguez-Sola et al., 2015), and for the survival of mature B cells in the context of "tonic" BCR signaling (Srinivasan et al., 2009). Importantly, the use of PI3K and AKT inhibitors on WT mature B cells in vitro allowed us to further demonstrate that inhibition of the PI3K/AKT pathway in these cells induced Rag1/2 expression. Our data suggest that in normal mature splenic B cells, miRNAs regulate PTEN levels and possibly FOXO1 (whose 3′UTRs contain putative binding sites for miRNAs expressed in B cells). PTEN is a known target of several miRNAs, including miR-181, a miRNA highly expressed in B cells (Chen et al., 2004), during NKT cell development

(Henao-Mejia et al., 2013), and miR-148 during immature B cells (Gonzalez-Martin et al., 2016). The miR-17∼92 cluster has also been shown to regulate PTEN in several cell types (Xiao et al., 2008), in particular miR-19 might be regulating PTEN at the immature B cell stage (Benhamou et al., 2016; Lai et al., 2016). The present results indicate that in addition to its pro-survival activity in mature B cells, the PI3K/AKT-FOXO pathway is also critical for inhibiting aberrant *Rag1/2* expression and light chain rearrangement in mature B cells.

Regulation of RAG expression in splenic B cells is absolutely critical for preventing anomalous rearrangements that may otherwise contribute to lymphomagenesis (Deriano et al., 2011; Mills et al., 2003). However, additional levels of control, including nuclear localization (Hewitt et al., 2009; Hu et al., 2015), prevent fully rearranged *Ig* alleles from RAG-mediated recombination in mature B lymphocytes. We did not observe aberrant *IgH* rearrangement in *Dicer1*$^{fl/fl}$ *Mb1*-cre *EμBcl2*^{Tg} mice and did not detect loss of *IgL* in B lymphocytes from *Dicer*$^{fl/fl}$ *Mx1Cre* mice upon poly(I:C) injection. This could either be a reflection of *Ig* loci inaccessibility in B cells where deletion of miRNAs only occurs once the cells are fully mature or may be due to the limited lifespan of Ig^{low} cells in *Dicer*$^{fl/fl}$ *Mx1Cre* mice in the absence of the Bcl2 Tg.

Expression of EμBcl2^{Tg} together with the *IgHEL* transgene allowed a complete rescue of B cell development in *Dicer1*$^{fl/fl}$ *Mb1*-cre. We observed normal Ig expression on the surface of the rescued B lymphocytes expressing the *IgHEL* transgene that encodes both *IgH* and *IgL* chains of a functional BCR specific for hen egg lysozyme (HEL) and that is not amenable to receptor editing. Importantly, the *IgHEL* Tg by itself only partially rescued B cell development in the absence of Dicer (Koralov et al., 2008). The nearly complete rescue of RNAi-deficient B cells by the combination of a pro-survival Bcl2 and pre-rearranged *Ig* Tg suggests that miRNAs regulate both cellular survival and *Ig* light chain recombination during B cell development. Our analysis of miRNA-deficient B cells suggests that by regulating levels of PTEN, AKT, and FOXO1, miRNAs function in B lymphocytes to regulate proliferation, survival, and to prevent aberrant V(D)J rearrangement.

EXPERIMENTAL PROCEDURES

Flow Cytometry and Cell Sorting

Single cell suspensions from spleen or bone marrow were stained for surface or intracellular markers. Samples were analyzed on a LSR Fortessa cytometer or sorted using a FACS Aria (BD Biosciences) or MoFlo (Beckman Coulter). Data were analyzed with FlowJo software (Tree Star). A detailed description is provided in the Supplemental Experimental Procedures.

miRNA and Gene Expression Analysis by Real-Time PCR

Total RNA was extracted using mirVana miRNA Isolation Kit (Ambion). TaqMan microRNA assays (Applied Biosystems) were used for reverse transcription and detection of miRNA levels. The small RNA U6 was used for normalization. Further isolation of longer RNAs was done by RNA cleanup using the RNeasy Micro kit (QIAGEN). cDNA was synthesized from mRNA using SuperScript VILO (Invitrogen). Real-time PCR was performed using a StepOne Plus PCR system using SybrGreen master mix (Applied Biosystems). The expression of target mRNA was calculated and normalized to the expression of the housekeeping gene *Hprt*. The list of the primers used is described in the Supplemental Experimental Procedures.

Analysis of *IgL* Rearrangement by Real-Time PCR and Sequencing

Genomic DNA (gDNA) was isolated from sorted cells by proteinase K digestion in Tris buffer at 56°C ∼4 hr. gDNA was then used for real-time PCR analysis. Levels were normalized to λ5 genomic region. The list of the primers used is described in the Supplemental Experimental Procedures. For sequencing of *Igκ* rearrangements, RNA was isolated from sorted cells and cDNA was prepared. *VκJκ* joints were amplified by PCR with high-fidelity Taq enzyme (Roche) using a degenerate Vk primer, 5′-agcttcagtggcagtgg(g/a)tc(a/t)gg(g/a)ac-3′, with a Ck primer, 5′-cttccacttgacattgatgtc-3′. PCR products were subcloned into pgem T Easy Vector (Promega) and sequenced. Unique sequences were analyzed using NCBI IgBlast program (http://www.ncbi.nlm.nih.gov/igblast).

Statistical Analysis

Statistical analyses were performed using Prism 5.0 (GraphPad Software). Data were analyzed with a Mann-Whitney test. A p value of <0.05 was considered significant. Immuno-FISH statistical analyses were performed using a two-tail Fisher's exact test: p values ≤ 0.05 were taken to be significant. P values displayed in the main figure were applied to combined data from repeated experiments.

SUPPLEMENTAL INFORMATION

Supplemental Information includes Supplemental Experimental Procedures, six figures, and one table and can be found with this article online at http://dx.doi.org/10.1016/j.celrep.2016.11.006.

AUTHOR CONTRIBUTIONS

M.C. and S.B.K. performed and designed experiments, analyzed the data, and wrote the manuscript. D.B., D.R., L.B., V.S., M.J.H., T.C., S.B., K.J., and L.G. performed experiments and/or contributed to analysis. M.M.W.C., R.B., D.R.L., and D.C. generated gene-targeted animals used for this project and provided scientific input. G.J.S., D.M., J.A.S., and K.R. designed experiments and participated in the preparation of the manuscript.

ACKNOWLEDGMENTS

We thank Dr. Pelanda for sharing the AKT/pAKT staining protocol with us. We thank Pedro Rocha for his help with ImmunoFISH analysis. We thank NYU Medical Center Cytometry and Cell Sorting Core for assistance. We thank all members of the Koralov lab for regular discussions of the presented results. We apologize to authors whose work we could not cite due to space constraints. Koralov lab is grateful for support from NIAID (R21AI110830-01), Beckman Foundation, and Ralph S. French Charitable Trust. K.R. was funded by NIH (1R01AI064345-01) and the European Research Council (Advanced Grant 268921) and D.M. lab was funded by The Israel Science Foundation (1408/13).

Received: July 12, 2016
Revised: September 14, 2016
Accepted: October 26, 2016
Published: November 22, 2016

REFERENCES

Alt, F.W., Bothwell, A.L., Knapp, M., Siden, E., Mather, E., Koshland, M., and Baltimore, D. (1980). Synthesis of secreted and membrane-bound immunoglobulin mu heavy chains is directed by mRNAs that differ at their 3′ ends. Cell *20*, 293–301.

Amin, R.H., and Schlissel, M.S. (2008). Foxo1 directly regulates the transcription of recombination-activating genes during B cell development. Nat. Immunol. *9*, 613–622.

Babiarz, J.E., Ruby, J.G., Wang, Y., Bartel, D.P., and Blelloch, R. (2008). Mouse ES cells express endogenous shRNAs, siRNAs, and other

Microprocessor-independent, Dicer-dependent small RNAs. Genes Dev. *22*, 2773–2785.

Belver, L., de Yébenes, V.G., and Ramiro, A.R. (2010). MicroRNAs prevent the generation of autoreactive antibodies. Immunity *33*, 713–722.

Benhamou, D., Labi, V., Novak, R., Dai, I., Shafir-Alon, S., Weiss, A., Gaujoux, R., Arnold, R., Shen-Orr, S.S., Rajewsky, K., and Melamed, D. (2016). A c-Myc/miR17-92/Pten axis controls PI3K-mediated positive and negative selection in B cell development and reconstitutes CD19 deficiency. Cell Rep. *16*, 419–431.

Busslinger, M. (2004). Transcriptional control of early B cell development. Annu. Rev. Immunol. *22*, 55–79.

Castel, S.E., and Martienssen, R.A. (2013). RNA interference in the nucleus: roles for small RNAs in transcription, epigenetics and beyond. Nat. Rev. Genet. *14*, 100–112.

Chen, C.Z., Li, L., Lodish, H.F., and Bartel, D.P. (2004). MicroRNAs modulate hematopoietic lineage differentiation. Science *303*, 83–86.

Chong, M.M., Rasmussen, J.P., Rudensky, A.Y., and Littman, D.R. (2008). The RNAseIII enzyme Drosha is critical in T cells for preventing lethal inflammatory disease. J. Exp. Med. *205*, 2005–2017.

Dengler, H.S., Baracho, G.V., Omori, S.A., Bruckner, S., Arden, K.C., Castrillon, D.H., DePinho, R.A., and Rickert, R.C. (2008). Distinct functions for the transcription factor Foxo1 at various stages of B cell differentiation. Nat. Immunol. *9*, 1388–1398.

Deriano, L., Chaumeil, J., Coussens, M., Multani, A., Chou, Y., Alekseyenko, A.V., Chang, S., Skok, J.A., and Roth, D.B. (2011). The RAG2 C terminus suppresses genomic instability and lymphomagenesis. Nature *471*, 119–123.

Di Lisio, L., Martinez, N., Montes-Moreno, S., Piris-Villaespesa, M., Sanchez-Beato, M., and Piris, M.A. (2012). The role of miRNAs in the pathogenesis and diagnosis of B-cell lymphomas. Blood *120*, 1782–1790.

Diamant, E., Keren, Z., and Melamed, D. (2005). CD19 regulates positive selection and maturation in B lymphopoiesis: lack of CD19 imposes developmental arrest of immature B cells and consequential stimulation of receptor editing. Blood *105*, 3247–3254.

Dominguez-Sola, D., Kung, J., Holmes, A.B., Wells, V.A., Mo, T., Basso, K., and Dalla-Favera, R. (2015). The FOXO1 Transcription Factor Instructs the Germinal Center Dark Zone Program. Immunity *43*, 1064–1074.

Early, P., Rogers, J., Davis, M., Calame, K., Bond, M., Wall, R., and Hood, L. (1980). Two mRNAs can be produced from a single immunoglobulin mu gene by alternative RNA processing pathways. Cell *20*, 313–319.

Ender, C., Krek, A., Friedländer, M.R., Beitzinger, M., Weinmann, L., Chen, W., Pfeffer, S., Rajewsky, N., and Meister, G. (2008). A human snoRNA with microRNA-like functions. Mol. Cell *32*, 519–528.

Fragoso, R., Mao, T., Wang, S., Schaffert, S., Gong, X., Yue, S., Luong, R., Min, H., Yashiro-Ohtani, Y., Davis, M., et al. (2012). Modulating the strength and threshold of NOTCH oncogenic signals by mir-181a-1/b-1. PLoS Genet. *8*, e1002855.

Gonzalez-Martin, A., Adams, B.D., Lai, M., Shepherd, J., Salvador-Bernaldez, M., Salvador, J.M., Lu, J., Nemazee, D., and Xiao, C. (2016). The microRNA miR-148a functions as a critical regulator of B cell tolerance and autoimmunity. Nat. Immunol. *17*, 433–440.

Goodnow, C.C., Crosbie, J., Adelstein, S., Lavoie, T.B., Smith-Gill, S.J., Brink, R.A., Pritchard-Briscoe, H., Wotherspoon, J.S., Loblay, R.H., Raphael, K., et al. (1988). Altered immunoglobulin expression and functional silencing of self-reactive B lymphocytes in transgenic mice. Nature *334*, 676–682.

Han, S., Dillon, S.R., Zheng, B., Shimoda, M., Schlissel, M.S., and Kelsoe, G. (1997). V(D)J recombinase activity in a subset of germinal center B lymphocytes. Science *278*, 301–305.

He, L., Thomson, J.M., Hemann, M.T., Hernando-Monge, E., Mu, D., Goodson, S., Powers, S., Cordon-Cardo, C., Lowe, S.W., Hannon, G.J., and Hammond, S.M. (2005). A microRNA polycistron as a potential human oncogene. Nature *435*, 828–833.

Henao-Mejia, J., Williams, A., Goff, L.A., Staron, M., Licona-Limón, P., Kaech, S.M., Nakayama, M., Rinn, J.L., and Flavell, R.A. (2013). The microRNA miR-181 is a critical cellular metabolic rheostat essential for NKT cell ontogenesis and lymphocyte development and homeostasis. Immunity *38*, 984–997.

Herzog, S., Hug, E., Meixlsperger, S., Paik, J.H., DePinho, R.A., Reth, M., and Jumaa, H. (2008). SLP-65 regulates immunoglobulin light chain gene recombination through the PI(3)K-PKB-Foxo pathway. Nat. Immunol. *9*, 623–631.

Hewitt, S.L., Yin, B., Ji, Y., Chaumeil, J., Marszalek, K., Tenthorey, J., Salvagiotto, G., Steinel, N., Ramsey, L.B., Ghysdael, J., et al. (2009). RAG-1 and ATM coordinate monoallelic recombination and nuclear positioning of immunoglobulin loci. Nat. Immunol. *10*, 655–664.

Hikida, M., Mori, M., Takai, T., Tomochika, K., Hamatani, K., and Ohmori, H. (1996). Reexpression of RAG-1 and RAG-2 genes in activated mature mouse B cells. Science *274*, 2092–2094.

Hobeika, E., Thiemann, S., Storch, B., Jumaa, H., Nielsen, P.J., Pelanda, R., and Reth, M. (2006). Testing gene function early in the B cell lineage in mb1-cre mice. Proc. Natl. Acad. Sci. USA *103*, 13789–13794.

Hu, J., Zhang, Y., Zhao, L., Frock, R.L., Du, Z., Meyers, R.M., Meng, F.L., Schatz, D.G., and Alt, F.W. (2015). Chromosomal loop domains direct the recombination of antigen receptor genes. Cell *163*, 947–959.

Koralov, S.B., Novobrantseva, T.I., Hochedlinger, K., Jaenisch, R., and Rajewsky, K. (2005). Direct in vivo VH to JH rearrangement violating the 12/23 rule. J. Exp. Med. *201*, 341–348.

Koralov, S.B., Muljo, S.A., Galler, G.R., Krek, A., Chakraborty, T., Kanellopoulou, C., Jensen, K., Cobb, B.S., Merkenschlager, M., Rajewsky, N., and Rajewsky, K. (2008). Dicer ablation affects antibody diversity and cell survival in the B lymphocyte lineage. Cell *132*, 860–874.

Krol, J., Loedige, I., and Filipowicz, W. (2010). The widespread regulation of microRNA biogenesis, function and decay. Nat. Rev. Genet. *11*, 597–610.

Kuchen, S., Resch, W., Yamane, A., Kuo, N., Li, Z., Chakraborty, T., Wei, L., Laurence, A., Yasuda, T., Peng, S., et al. (2010). Regulation of microRNA expression and abundance during lymphopoiesis. Immunity *32*, 828–839.

Kühn, R., Schwenk, F., Aguet, M., and Rajewsky, K. (1995). Inducible gene targeting in mice. Science *269*, 1427–1429.

Lai, M., Gonzalez-Martin, A., and Cooper, A.B. (2016). Regulation of B-cell development and tolerance by different members of the miR-17∼92 family microRNAs. Nat. Commun. *7*, 12207.

Landgraf, P., Rusu, M., Sheridan, R., Sewer, A., Iovino, N., Aravin, A., Pfeffer, S., Rice, A., Kamphorst, A.O., Landthaler, M., et al. (2007). A mammalian microRNA expression atlas based on small RNA library sequencing. Cell *129*, 1401–1414.

Lang, J., Arnold, B., Hammerling, G., Harris, A.W., Korsmeyer, S., Russell, D., Strasser, A., and Nemazee, D. (1997). Enforced Bcl-2 expression inhibits antigen-mediated clonal elimination of peripheral B cells in an antigen dose-dependent manner and promotes receptor editing in autoreactive, immature B cells. J. Exp. Med. *186*, 1513–1522.

Lim, L.P., Glasner, M.E., Yekta, S., Burge, C.B., and Bartel, D.P. (2003). Vertebrate microRNA genes. Science *299*, 1540.

Lim, L.P., Lau, N.C., Garrett-Engele, P., Grimson, A., Schelter, J.M., Castle, J., Bartel, D.P., Linsley, P.S., and Johnson, J.M. (2005). Microarray analysis shows that some microRNAs downregulate large numbers of target mRNAs. Nature *433*, 769–773.

Miletic, A.V., Anzelon-Mills, A.N., Mills, D.M., Omori, S.A., Pedersen, I.M., Shin, D.M., Ravetch, J.V., Bolland, S., Morse, H.C., 3rd, and Rickert, R.C. (2010). Coordinate suppression of B cell lymphoma by PTEN and SHIP phosphatases. J. Exp. Med. *207*, 2407–2420.

Mills, K.D., Ferguson, D.O., and Alt, F.W. (2003). The role of DNA breaks in genomic instability and tumorigenesis. Immunol. Rev. *194*, 77–95.

Mu, P., Han, Y.C., Betel, D., Yao, E., Squatrito, M., Ogrodowski, P., de Stanchina, E., D'Andrea, A., Sander, C., and Ventura, A. (2009). Genetic dissection of the miR-17∼92 cluster of microRNAs in Myc-induced B-cell lymphomas. Genes Dev. *23*, 2806–2811.

Murchison, E.P., Partridge, J.F., Tam, O.H., Cheloufi, S., and Hannon, G.J. (2005). Characterization of Dicer-deficient murine embryonic stem cells. Proc. Natl. Acad. Sci. USA *102*, 12135–12140.

Nishi, M., Kataoka, T., and Honjo, T. (1985). Preferential rearrangement of the immunoglobulin kappa chain joining region J kappa 1 and J kappa 2 segments in mouse spleen DNA. Proc. Natl. Acad. Sci. USA *82*, 6399–6403.

Okamura, K., and Lai, E.C. (2008). Endogenous small interfering RNAs in animals. Nat. Rev. Mol. Cell Biol. *9*, 673–678.

Pauli, A., Rinn, J.L., and Schier, A.F. (2011). Non-coding RNAs as regulators of embryogenesis. Nat. Rev. Genet. *12*, 136–149.

Peled, J.U., Kuang, F.L., Iglesias-Ussel, M.D., Roa, S., Kalis, S.L., Goodman, M.F., and Scharff, M.D. (2008). The biochemistry of somatic hypermutation. Annu. Rev. Immunol. *26*, 481–511.

Rajewsky, K. (1996). Clonal selection and learning in the antibody system. Nature *381*, 751–758.

Rao, D.S., O'Connell, R.M., Chaudhuri, A.A., Garcia-Flores, Y., Geiger, T.L., and Baltimore, D. (2010). MicroRNA-34a perturbs B lymphocyte development by repressing the forkhead box transcription factor Foxp1. Immunity *33*, 48–59.

Rogers, J., Early, P., Carter, C., Calame, K., Bond, M., Hood, L., and Wall, R. (1980). Two mRNAs with different 3′ ends encode membrane-bound and secreted forms of immunoglobulin mu chain. Cell *20*, 303–312.

Ruby, J.G., Jan, C.H., and Bartel, D.P. (2007). Intronic microRNA precursors that bypass Drosha processing. Nature *448*, 83–86.

Sander, S., Chu, V.T., Yasuda, T., Franklin, A., Graf, R., Calado, D.P., Li, S., Imami, K., Selbach, M., Di Virgilio, M., et al. (2015). PI3 Kinase and FOXO1 Transcription Factor Activity Differentially Control B Cells in the Germinal Center Light and Dark Zones. Immunity *43*, 1075–1086.

Sarbassov, D.D., Guertin, D.A., Ali, S.M., and Sabatini, D.M. (2005). Phosphorylation and regulation of Akt/PKB by the rictor-mTOR complex. Science *307*, 1098–1101.

Seong, Y., Lim, D.H., Kim, A., Seo, J.H., Lee, Y.S., Song, H., and Kwon, Y.S. (2014). Global identification of target recognition and cleavage by the Microprocessor in human ES cells. Nucleic Acids Res. *42*, 12806–12821.

Spierings, D.C., McGoldrick, D., Hamilton-Easton, A.M., Neale, G., Murchison, E.P., Hannon, G.J., Green, D.R., and Withoff, S. (2011). Ordered progression of stage-specific miRNA profiles in the mouse B2 B-cell lineage. Blood *117*, 5340–5349.

Srinivasan, L., Sasaki, Y., Calado, D.P., Zhang, B., Paik, J.H., DePinho, R.A., Kutok, J.L., Kearney, J.F., Otipoby, K.L., and Rajewsky, K. (2009). PI3 kinase signals BCR-dependent mature B cell survival. Cell *139*, 573–586.

Stavnezer, J., Guikema, J.E., and Schrader, C.E. (2008). Mechanism and regulation of class switch recombination. Annu. Rev. Immunol. *26*, 261–292.

Stephens, L., Anderson, K., Stokoe, D., Erdjument-Bromage, H., Painter, G.F., Holmes, A.B., Gaffney, P.R., Reese, C.B., McCormick, F., Tempst, P., et al. (1998). Protein kinase B kinases that mediate phosphatidylinositol 3,4,5-trisphosphate-dependent activation of protein kinase B. Science *279*, 710–714.

Strasser, A., Whittingham, S., Vaux, D.L., Bath, M.L., Adams, J.M., Cory, S., and Harris, A.W. (1991). Enforced BCL2 expression in B-lymphoid cells prolongs antibody responses and elicits autoimmune disease. Proc. Natl. Acad. Sci. USA *88*, 8661–8665.

Sudo, T., Nishikawa, S., Ohno, N., Akiyama, N., Tamakoshi, M., Yoshida, H., and Nishikawa, S. (1993). Expression and function of the interleukin 7 receptor in murine lymphocytes. Proc. Natl. Acad. Sci. USA *90*, 9125–9129.

Sun, H., Lesche, R., Li, D.M., Liliental, J., Zhang, H., Gao, J., Gavrilova, N., Mueller, B., Liu, X., and Wu, H. (1999). PTEN modulates cell cycle progression and cell survival by regulating phosphatidylinositol 3,4,5,-trisphosphate and Akt/protein kinase B signaling pathway. Proc. Natl. Acad. Sci. USA *96*, 6199–6204.

Tzivion, G., Dobson, M., and Ramakrishnan, G. (2011). FoxO transcription factors; Regulation by AKT and 14-3-3 proteins. Biochim. Biophys. Acta *1813*, 1938–1945.

Vela, J.L., Aït-Azzouzene, D., Duong, B.H., Ota, T., and Nemazee, D. (2008). Rearrangement of mouse immunoglobulin kappa deleting element recombining sequence promotes immune tolerance and lambda B cell production. Immunity *28*, 161–170.

Ventura, A., Young, A.G., Winslow, M.M., Lintault, L., Meissner, A., Erkeland, S.J., Newman, J., Bronson, R.T., Crowley, D., Stone, J.R., et al. (2008). Targeted deletion reveals essential and overlapping functions of the miR-17 through 92 family of miRNA clusters. Cell *132*, 875–886.

Verkoczy, L., Duong, B., Skog, P., Aït-Azzouzene, D., Puri, K., Vela, J.L., and Nemazee, D. (2007). Basal B cell receptor-directed phosphatidylinositol 3-kinase signaling turns off RAGs and promotes B cell-positive selection. J. Immunol. *178*, 6332–6341.

Wang, Y., Medvid, R., Melton, C., Jaenisch, R., and Blelloch, R. (2007). DGCR8 is essential for microRNA biogenesis and silencing of embryonic stem cell self-renewal. Nat. Genet. *39*, 380–385.

Werner, M., Hobeika, E., and Jumaa, H. (2010). Role of PI3K in the generation and survival of B cells. Immunol. Rev. *237*, 55–71.

Wilson, R.C., and Doudna, J.A. (2013). Molecular mechanisms of RNA interference. Annu. Rev. Biophys. *42*, 217–239.

Winter, J., Jung, S., Keller, S., Gregory, R.I., and Diederichs, S. (2009). Many roads to maturity: microRNA biogenesis pathways and their regulation. Nat. Cell Biol. *11*, 228–234.

Xiao, C., Calado, D.P., Galler, G., Thai, T.H., Patterson, H.C., Wang, J., Rajewsky, N., Bender, T.P., and Rajewsky, K. (2007). MiR-150 controls B cell differentiation by targeting the transcription factor c-Myb. Cell *131*, 146–159.

Xiao, C., Srinivasan, L., Calado, D.P., Patterson, H.C., Zhang, B., Wang, J., Henderson, J.M., Kutok, J.L., and Rajewsky, K. (2008). Lymphoproliferative disease and autoimmunity in mice with increased miR-17-92 expression in lymphocytes. Nat. Immunol. *9*, 405–414.

Xu, S., Guo, K., Zeng, Q., Huo, J., and Lam, K.P. (2012). The RNase III enzyme Dicer is essential for germinal center B-cell formation. Blood *119*, 767–776.

Zhou, B., Wang, S., Mayr, C., Bartel, D.P., and Lodish, H.F. (2007). miR-150, a microRNA expressed in mature B and T cells, blocks early B cell development when expressed prematurely. Proc. Natl. Acad. Sci. USA *104*, 7080–7085.

Cell Reports, Volume *17*

Supplemental Information

miRNAs Are Essential for the Regulation of the PI3K/AKT/FOXO Pathway and Receptor Editing during B Cell Maturation

Maryaline Coffre, David Benhamou, David Rieß, Lili Blumenberg, Valentina Snetkova, Marcus J. Hines, Tirtha Chakraborty, Sofia Bajwa, Kari Jensen, Mark M.W. Chong, Lelise Getu, Gregg J. Silverman, Robert Blelloch, Dan R. Littman, Dinis Calado, Doron Melamed, Jane A. Skok, Klaus Rajewsky, and Sergei B. Koralov

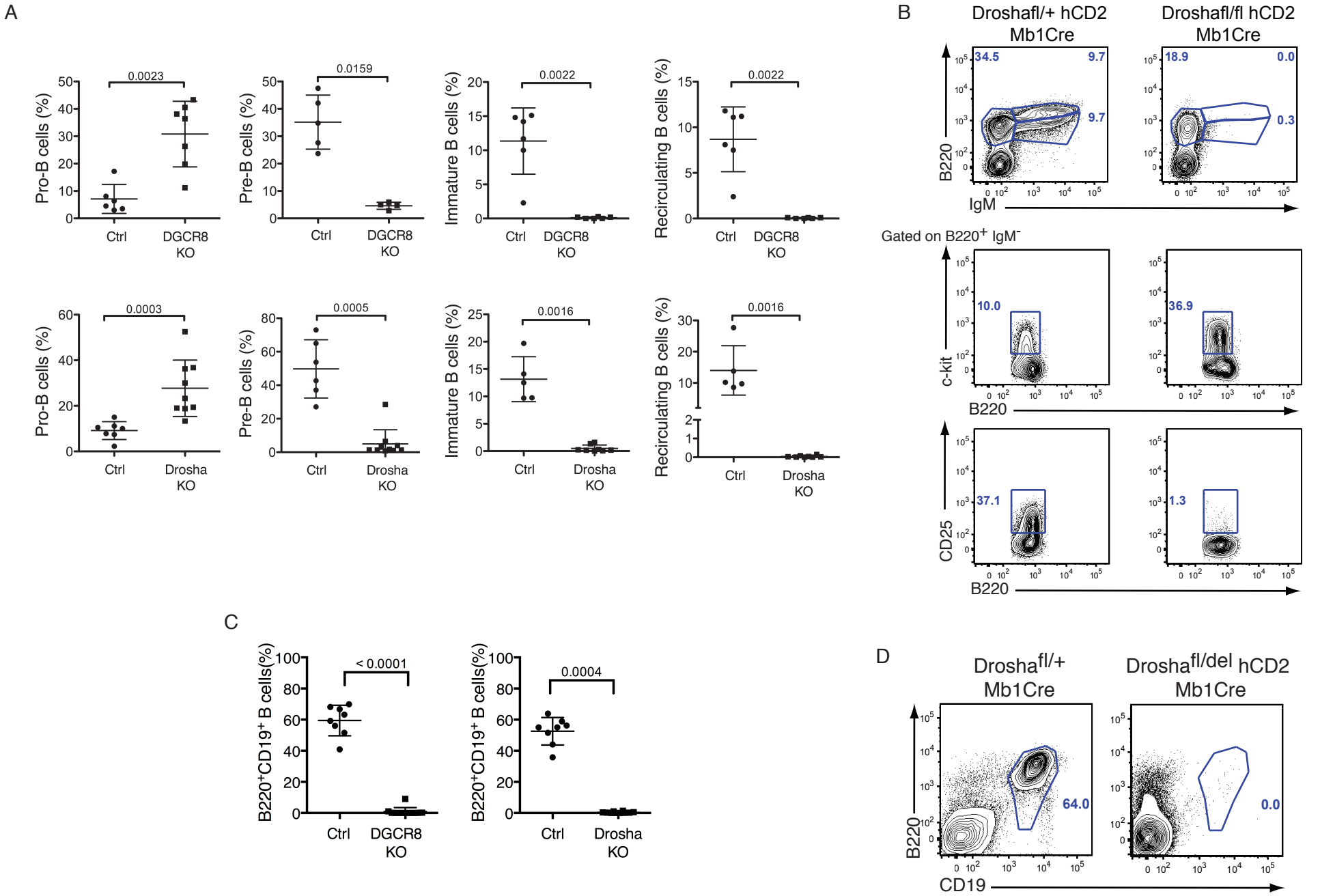

Figure S1, related to Figure 1: Block in early B cell development in absence of DGCR8 and Drosha.
(A) Percentage of Pro-B ($B220^{+}IgM^{-}c\text{-}kit^{+}$), Pre-B ($B220^{+}IgM^{-}CD25^{+}$), Immature ($B220^{Int}IgM^{+}$) and recirculating ($B220^{Hi}IgM^{+}$) B cells in the bone marrow of *Dgcr8*$^{fl/fl}$ *Mb1*-cre (DGCR8 KO), *Drosha*$^{fl/fl}$ *Mb1*-Cre (Drosha KO) or the appropriate control (ctrl) mice (mean ±SD). P-values <0.05 are indicated. (B) Representative FACS plots of bone marrow from *Drosha*$^{fl/fl}$ R26hCD2$^{stopfl/+}$ *Mb1*-cre and *Drosha*$^{fl/+}$ R26hCD2$^{stopfl/+}$ *Mb1*-cre control animals. Events are gated on total lymphocytes. Plots showing pro-B cells ($B220^{+}c\text{-}kit^{+}$) and pre-B cells ($B220^{+}CD25^{+}$) cells are gated on $B220^{+}$ IgM^{-} B lymphocyte progenitor cells (n≥5 mice). (C) Percentage of $B220^{+}CD19^{+}$ B cells in the spleen of the indicated mice (mean ±SD). P-values <0.05 are indicated. (D) Representative FACS plots of spleen from *Drosha*$^{fl/fl}$ R26hCD2$^{stopfl/+}$ *Mb1*-cre and *Drosha*$^{fl/+}$ *Mb1*-cre mice. Events are gated on total lymphocytes (n≥5 mice).

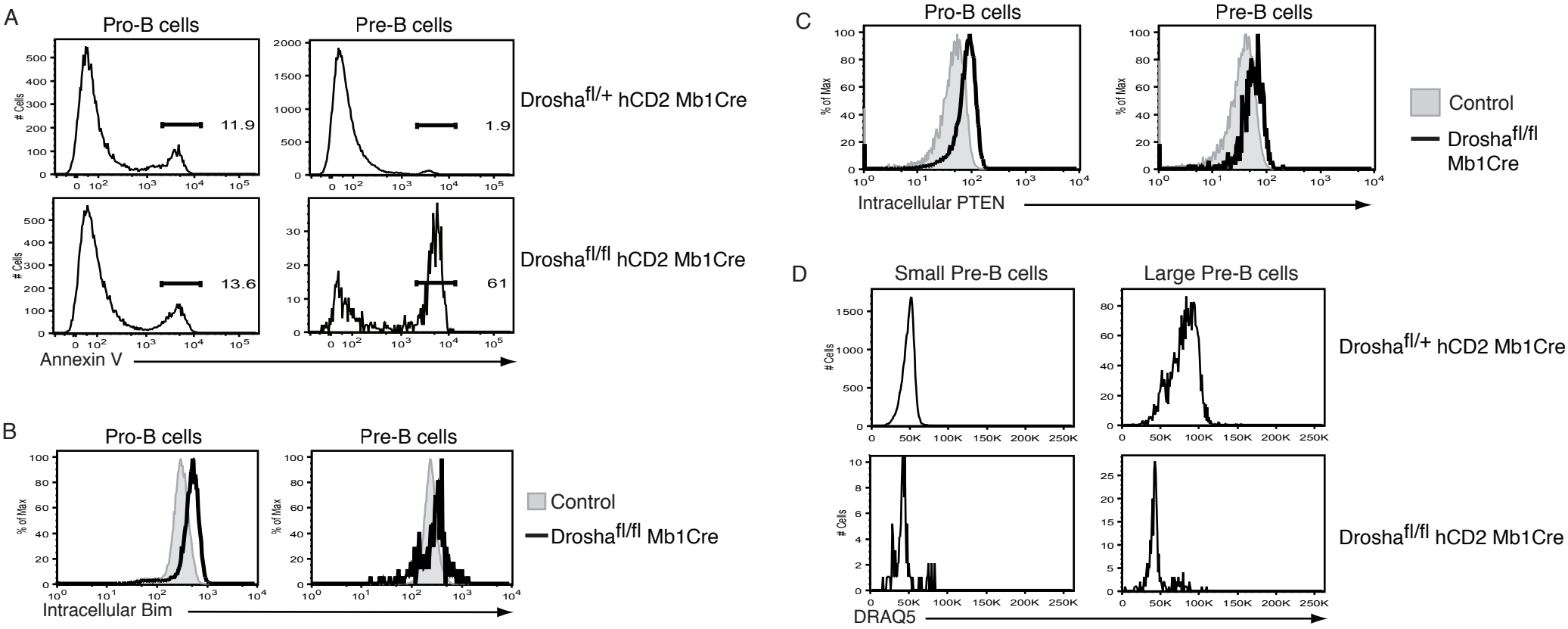

Figure S2, related to Figure 1: Survival and proliferation defects in Drosha-deficient pre-B cells

(A) Representative Annexin V staining of pro-B and pre-B cells gated as in Figure S1B from mice of the indicated genotypes. Representative histograms for intracellular Bim (B) and PTEN (C) staining on pro-B and pre-B cells gated as in Figure S1B from *Drosha*$^{fl/fl}$ *Mb1*-cre (solid line) or control (shaded) mice. (D) DRAQ5 incorporation into small or large pre-B cells (gated on B220^{+}IgM^{-}CD25^{-} then gated on size) (n≥5 mice).

A

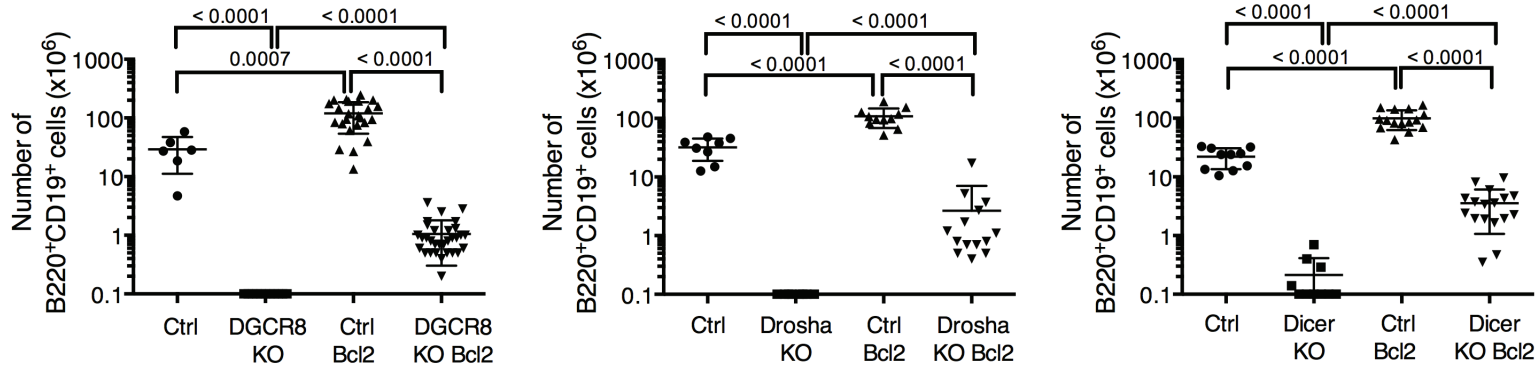

B

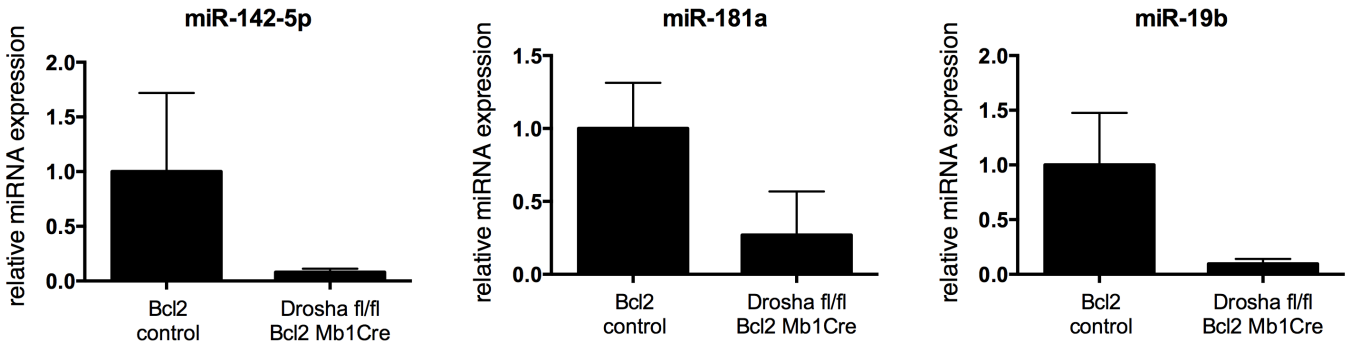

Figure S3, related to Figure 3: Partial rescue of miRNAs deficient B cells by a Bcl2 transgene
(A) Absolute number of B220^{+}CD19^{+} B cells in the spleen of *Dgcr8$^{fl/fl}$ Mb1*-cre (DGCR8 KO), *Dgcr8$^{fl/fl}$ Mb1*-cre EμBcl2Tg (DGCR8 KO Bcl2), or *Drosha$^{fl/fl}$ Mb1*-Cre (Drosha KO), or *Drosha$^{fl/fl}$ Mb1*-Cre EμBcl2Tg (Drosha KO Bcl2), or *Dicer1$^{fl/fl}$ Mb1-cre* (Dicer KO), *Dicer1$^{fl/fl}$ Mb1*-cre EμBcl2Tg (Dicer KO Bcl2). Ctrl and Ctrl Bcl2 indicate the appropriate control mice without and with Bcl2 respectively. Each dot is representative of one mouse (mean ±SD). P-values <0.05 are indicated. (n≥8 for each genotype). (B) Loss of miRNAs in *Drosha$^{fl/fl}$ Mb1*-cre EμBcl2Tg mice is shown by real-time PCR of a representative set of miRNAs on sorted B cells from the indicated mice. Taqman quantification of individual miRNAs was normalized against U6 and represented relative to the control cells, n≥2 for both groups (mean ±SD).

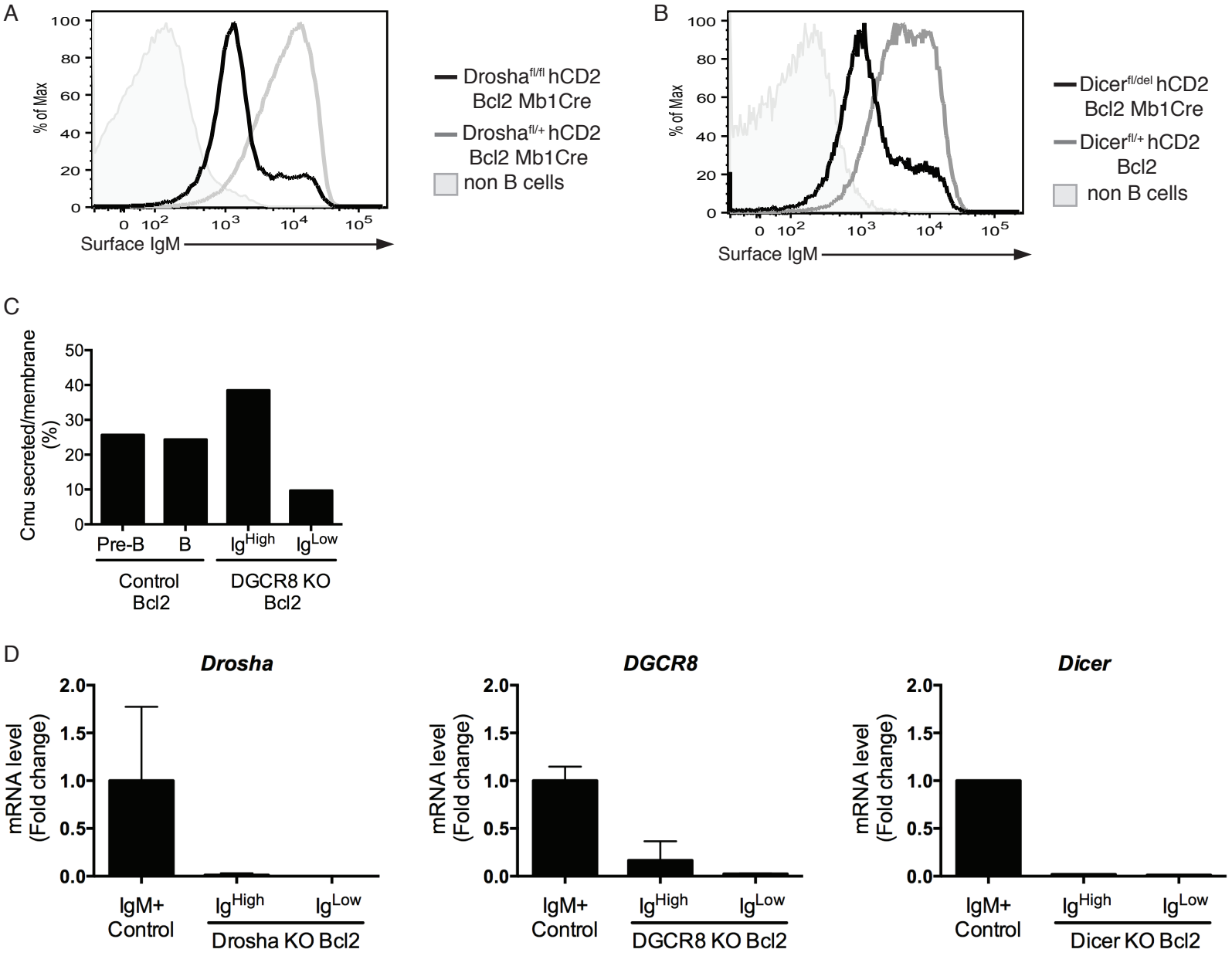

Figure S4, related to Figure 4: Two populations of Bcl2 rescued RNAi deficient B cells according to IgM surface levels
Surface IgM levels of B220^{+}CD19^{+} B cells from the spleen of *Drosha*$^{fl/fl}$ R26hCD2$^{stopfl/+}$ *Mb1*-cre EμBcl2Tg (black histogram) and *Drosha*$^{fl/+}$ R26hCD2$^{stopfl/+}$ *Mb1*-cre mice (grey histogram) (A) or *Dicer*$^{fl/del}$ R26hCD2$^{stopfl/+}$ *Mb1*-cre EμBcl2Tg (black histogram) and *Dicer*$^{fl/+}$ R26hCD2$^{stopfl/+}$ EμBcl2Tg mice (grey histogram) (B). Non-B (B220^{-}CD19^{-}) lymphocytes were used as a staining control (shaded histogram). Data is representative of >15 independent experiments. (C) Ratio of secreted to membrane-bound Cμ splice variants in the indicated cells sorted from spleen. Data is normalized to *hprt* and represented as percent of levels of membrane Cμ in the same cells. (D) Levels of *Drosha*, *Dgcr8*, *Dicer* mRNA in the indicated cells sorted from spleen (mean ± SD). Data is normalized to *hprt*.

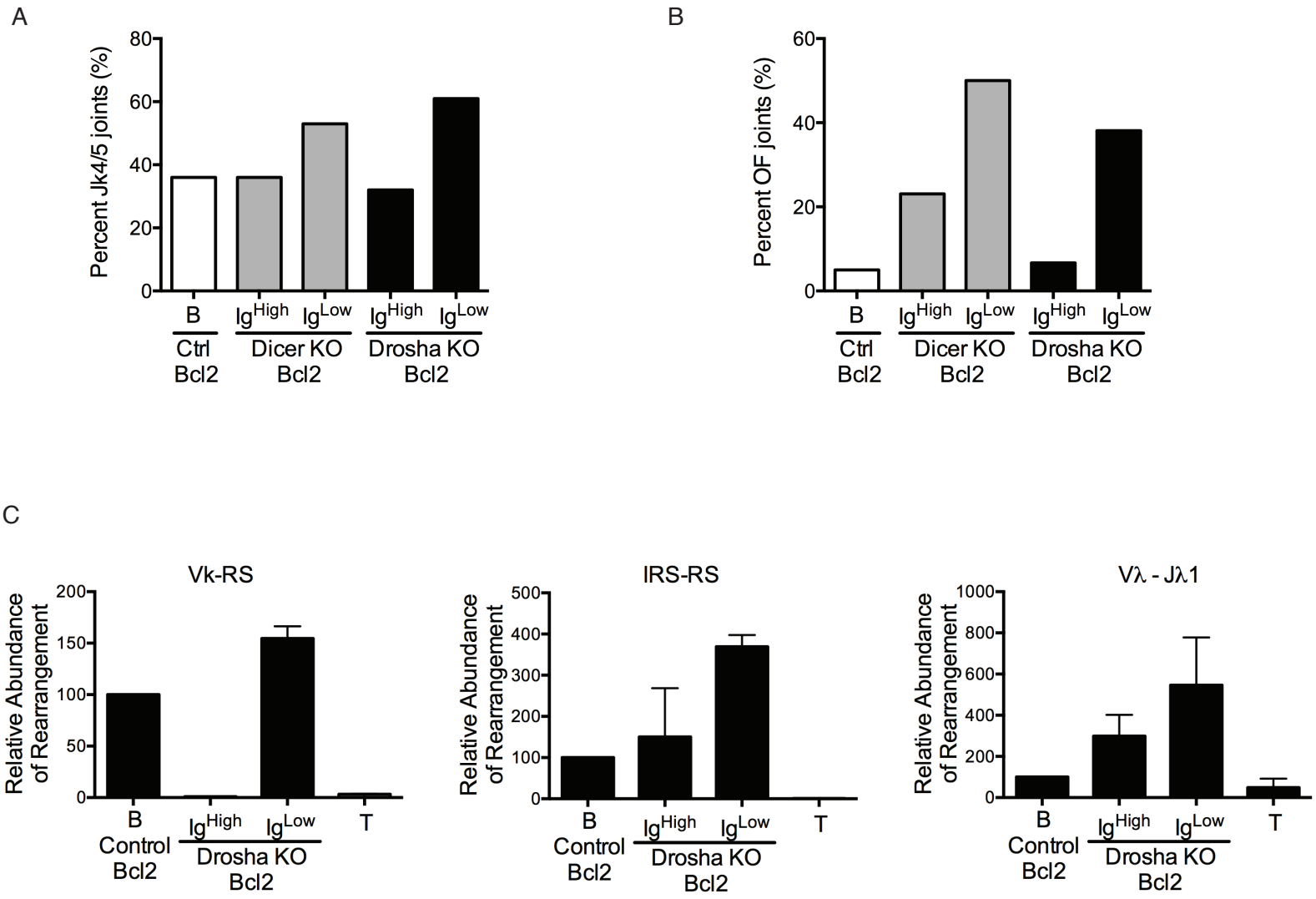

Figure S5, related to Figure 5: Igk joints in Ig^{low} cells

Splenic B220^{+}CD19^{+}CD25^{-} B cells *Dicer1*$^{fl/fl}$ *Mb1*-cre EμBcl2Tg (Dicer KO Bcl2) and *Drosha*$^{fl/fl}$ *Mb1*-Cre EμBcl2Tg (Drosha KO Bcl2) and Bcl2 expressing control (Ctrl Bcl2) were sorted according to surface IgM levels into Ig^{high} and Ig^{low} cells. Igκ light chain joints were sequenced and percent of Jκ4 and Jκ5 joints (A) or out-of-frame (OF) rearrangements (B) out of all Igκ joints were calculated. (C) Real-time PCR of Vκ-RS, IRS-RS and Vλ-Jλ1 joints in the gDNA of the indicated cells sorted as in (A). Data is normalized to λ5 and levels in control cells set as 100% (mean ± SD). T cells from control mice are used as a negative control.

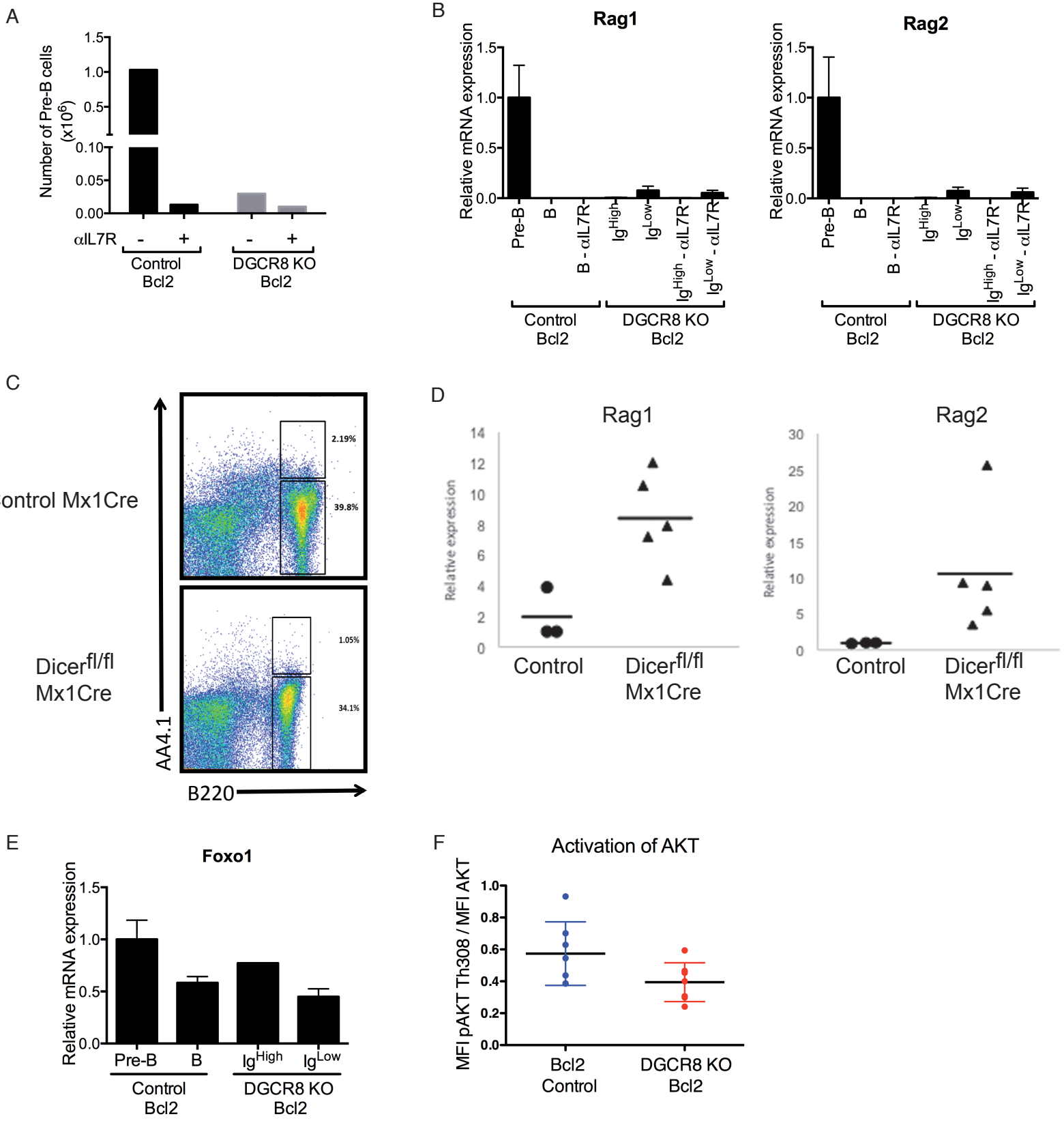

Figure S6, related to Figure 6: *Rag1/2* are expressed in RNAi deficient B cells

(A) Representative graph of absolute number of Pre-B ($B220^{+}IgM^{-}CD25^{+}$) from the BM of *Dgcr8*$^{fl/fl}$ *Mb1*-cre EμBcl2Tg (DGCR8 KO Bcl2) and Bcl2 expressing control mouse treated or not with anti-IL7Ra antibody. (B) Transcript levels of *Rag1* and *Rag2* were assessed in Ig^{high} or Ig^{low} splenic B cells deficient for DGCR8 (DGCR8 KO Bcl2) or in control B cells expressing Bcl2 Tg (Control Bcl2) treated or not with anti-IL-7R antibody. Data is normalized to *hprt* and represented as fold difference relative to Bcl2 Tg^{+} control pre-B cells. Values shown are mean ± SD. (C) FACS plots of B220 and AA4.1 (CD93) staining of the spleen *Dicer*$^{fl/fl}$ *Mx1*-Cre or Control *Mx1*-Cre mice one week after the last injection of poly(I:C). Number indicates the percentage of cells in the gate. (D) mRNA levels of *Rag1* and *Rag2* in *Dicer*$^{fl/fl}$ *Mx1*-Cre relative to control mice one week after poly(I:C) injection. (E) Levels of *Foxo1* mRNA in the indicated cells. Data is normalized to *hprt* and represented as fold difference relative to Bcl2 Tg^{+} control pre-B cells. Values shown are mean ± SD. (F) Ratio of the median fluorescence intensity (MFI) of phospho Th 308 AKT to total AKT MFI (mean ± SD; n=6 mice).

Table S1. Frequency of γ-H2AX colocalization with *Igk locus* (Related to Figure 5C)

Igk		No association number	%	γ-H2AX association number	%	sample size (cells)
PreB Bcl2	Exp1	30	56.6	23	43.4	53
Control	Exp2	65	68.4	30	31.6	95
	Total	**95**	**64.2**	**53**	**35.8**	**148**
B cell Bcl2	Exp1	56	93.3	4	6.7	60
Control	Exp2	94	94	6	6	100
	Total	**150**	**93.75**	**10**	**6.25**	**160**
B cell IgHigh	Exp1	56	94.9	3	5.1	59
Dicer KO Bcl2	Exp2	103	92.8	8	7.2	111
	Total	**170**	**93.5**	**11**	**6.5**	**170**
B cell Iglow	Exp1	51	82.2	11	17.7	62
Dicer KO Bcl2	Exp2	59	83.1	12	16.9	71
	Total	**110**	**82.7**	**23**	**17.3**	**133**
Statistical analysis (Fisher exact test)				*P*-value		Level
IgLow vs PreB Bcl2 Control				0,00048		***
Dicer KO Bcl2 B cell Control				0,0047		**
IgHigh Dicer KO Bcl2				0,0053		**

Supplemental Experimental Procedures

Animals

Mice carrying floxed alleles for *Dgcr8* (Wang et al., 2007) or *Drosha* (Chong et al., 2008) were bred with *Mb1-cre* animals (Hobeika et al., 2006) to generate *Dgcr8*$^{fl/fl}$ *Mb1*-cre, *Drosha*$^{fl/fl}$ *Mb1*-cre and littermate controls. *Dicer1*$^{fl/fl}$ *Mb1*-cre mice were previously described (Koralov et al., 2008). Animals heterozygous for any of the three floxed alleles and positive for *Mb1*-cre did not display any detectable phenotype and were used as controls together with littermates that carried either the appropriate floxed alleles or the *Mb1*-cre allele in the absence of the floxed alleles. In some experiments, these mice were bred to Eμ-bcl-2 transgenic mice (Strasser et al., 1990), to IgHEL transgenic mice (Goodnow et al., 1988), or to mice expressing a human CD2 reporter knocked into the Rosa 26 locus downstream of a floxed stop cassette (R26hCD2$^{stopfl/+}$)(Calado et al., 2012). Intraperitoneal injection of anti-IL7Ra antibody (A7R34; BioXcell) was performed every 3 days (0.5mg on day 1 then 0.25mg/injection) for two weeks. In some experiments, D*icer*$^{fl/fl}$ (Murchison et al., 2005) were bred with *Mx1*-cre transgenic mice (Kuhn et al., 1995). *In vivo* deletion of Dicer was obtained upon intraperitoneal injection of poly(I:C) on days 1, 4 and 7 (0.4 mg/injection). Mice were analyzed 7-10 days after last injection. Mice were housed and maintained in specific pathogen-free conditions at NYU School of Medicine, Jackson Laboratory and the Technion Faculty of Medicine (Israel) in accordance with protocols approved by the NYU and Technion Institutional Animal Care and Usage Committee. Mice were used between 6–10 weeks of age.

Flow Cytometry and Cell Sorting

For surface staining and cell sorting, single cell suspensions from spleen or bone marrow were stained 15 min on ice with antibodies specific to murine B220, CD19, c-kit, CD25, CD93 (AA4.1) (eBioscience), Igκ, Igλ (BD Biosciences) and IgM (μ chain specific) (Jackson ImmunoResearch). Dead cells were excluded by DAPI staining (Sigma). Annexin V staining was done according to manufacturer's protocol (eBioscience). For intracellular staining, cells were surface stained and fixation/permeabilisation buffers from eBioscience were used. Antibodies for intracellular staining were IgM, Igκ, Igλ (as mentioned above), Bim (Epitomics); PTEN, FOXO1 (Cell Signaling) followed by FITC conjugated anti-rabbit antibody (Jackson ImmunoResearch). For cell proliferation, cells were fixed and stained in 2% paraformaldehyde (PFA) for the DNA intercalent DRAQ 5 (Biostatus) following surface staining. For phosphoflow staining, cells were surface strained then fixed in 2% PFA for 30 min at RT and permeablized with 90% methanol for 30-60 min on ice. Cells were washed in PBS then stained for AKT, Phospho-AKT Thr308 and Phospho-AKT Ser473 (Cell Signaling) followed by APC-conjugated anti-rabbit antibody (Jackson ImmunoResearch).

Primers for gene expression Real-time PCR

The following primers were used:
Igll1 (lambda 5) forward 5'-CACATACTTTCCCCAAGCTC-3';
Igll1 (lambda 5) reverse 5'-GTGGGATGATCTGGAACAG-3';
VpreB forward 5'-CTATCTCACAGGTTGTGGC-3';
VpreB reverse 5'-GCCAATGTTATGGTCGTTG-3';
Drosha Forward 5'-GACGACGACAGCACCTGTT-3'as described in (Chong et al., 2008);
Drosha Rev 5'-GATAAATGCTGTGGCGGATT-3' as described in (Chong et al., 2008);
DGCR8 Forw2 5'-CTAGAAGAAGGTCTCTGTG-3';
DGCR8 Rev2 5'-GGTATACAGGGACTCCAG-3';
Dicer Forw2 5'-CTGATGCTCATGAAGGCC-3';
Dicer Rev2 5'-CCCACTTCTCTGAGTTAC-3';
FoxO1 Forw1 5'-GTGAAGAGCGTGCCCTAC-3'
FoxO1 Rev1 5'-GGATTGAGCATCCACCAAG-3'
Cmu Membrane(M1) FW 5'-GAGCCTCTTCTACAGCACCACC-3';
Cmu Membrane(M2) REV 5'-GTCATACAGTCAGGTATCCCAGG-3'
Cmu4 Forw 5'-CTATACCTGTGTTGTAGGCCAC-3';
CmuSecreted_Rev 5'-CTAGCATGGTCAATAGCAGGTGC-3';
RAG1 Fw: 5'-TTGCTATCTCTGTGGCATCG-3'
RAG1 Rv: 5'-AATTTCATCGGGTGCAGAAC-3'
RAG2 Fw: 5'-AGTGACTCTTCCCCAAGTGC-3'
RAG2 Rv: 5'-CTTCCTGCTTGTGGATGTGA-3'
HPRT1-E1-F: 5'-GTCATGCCGACCCGCAGTC-3'
HPRT1-E2-R: 5'-GTCCTGTCCATAATCAGTCCATGAGGAATAAAC-3'

Primers for *IgL* rearrangement RT-PCR

The following primers were used on genomic DNA
IRS forward: 5'-GTAGCATCCCTTGCTCCGCGTGG-3'
Vk forward: 5'-GCTTCAGTGGCAGTGGRTCWGGRAC-3'
RS Rev: 5'-ACATGGAAGTTTTCCTGGGAGAATATG-3'
Vlambda1 FW: 5'-ATCACAGGGGCACAGACTGAGG -3'

Jlambda: 15'-CTAGGACAGTCAGTTTGGTTCC-3'
Kappa Germline Forward: 5'-AGCTACCCACTGCTCTGTTC-3' as described in (Zhou et al., 2010)
Kappa Germline Reverse: 5'-CGTTTGATTTCCAGCTTGGT-3' as described in (Zhou et al., 2010)
Lambda 5 LOADING DNA Forward: 5'-TGCTGCTGTTGGGTCTAGTG-3'
Lambda 5 LOADING DNA Reverse: 5'-ACCTTCCCCAAAAAGCAAGT-3'

PI3K Inhibitors
Mature naïve B cells ($B220^+$ $CD19^+$ $AA4.1^-$) were sorted from WT C57/B6 mice. Cells were cultured in RPMI with L-glutamine (Corning) supplemented with 10% FBS (Hyclone), nonessential amino acids, 10 mM HEPES buffer, 1mM sodium pyruvate (Corning), penicillin-streptomycin (HyClone), and 0.1M 2-Mercaptoethanol (Sigma-Aldrich) at 37°C for the time indicated on the figure with DMSO, LY294002 (5μM or 10μM), PD98959 (10μM) (cell signaling), Wortmannin (10nM) or AKT inhibitor VIII (2mM) (Sigma-Aldrich).

Immunoblotting
BM and splenic B cells were FACS sorted and lysed in RIPA buffer containing 1 mM sodium orthovanadate and 5 mM sodiumfluoride and a protease inhibitor cocktail (Roche) for 15 minutes on ice. Proteins were resolved by SDS-Page and transferred to PVDF membranes (Millipore). Membranes were probed with antibodies specific to FOXO1. HRP-goat anti rabbit antibody was used as a secondary antibody, followed by detection using enhanced chemiluminescence (ThermoFisher). Membranes were stripped and probed with anti-histone H3 antibody as loading control. All antibodies used for immunoblotting were from Cell signaling.

DNA FISH with immunofluorescence (ImmunoFISH)
Sorted pre-B and splenic B cells were adhered to poly-L-lysine coated coverslips, and fixed for 10 min at 22°C with 2% (wt/vol) PFA in PBS and permeabilized for 5 min with 0.4% (vol/vol) Triton in PBS. Samples were blocked for 30 min with 2.5% (wt/vol) BSA, 10% (vol/vol) normal goat serum and 0.1% (vol/vol) Tween-20 in PBS at 22°C. Samples were incubated for 1 h at 22°C with an antibody to phosphorylated serine 139 of H2AX (γH2AX; JBW301, Millipore) in blocking solution followed by staining with secondary goat anti-mouse IgG Alexa Fluor 488 (Life Technologies). Cells were post-fixed for 5 min at 22°C in 1% (wt/vol) PFA, re-permeabilized for 10 min at 0°C in 0.7% (vol/vol) Triton-X-100 / 0.1 M HCl and incubated with RNaseA (0.1 mg/ml in PBS, 30 min at 37°C). Cells were then denatured for 30 min at 22°C with 1.9 M HCl and hybridized overnight at 37°C with denatured DNA probes. Cells were mounted in Prolong Gold (Life Technologies) containing 1.5μg/ml DAPI (Sigma). DNA probes were prepared by labeling BAC clones RPCI-24-387E13 (IgkC), RPCI-23-101G13 (IgkV) by nick translation with ChromaTide Alexa Fluor 488-5 or 594-5-dUTP (Life Technologies).

Confocal microscopy and ImmunoFISH analysis
Cells were imaged by confocal microscopy on a Leica SP5 AOBS system (Acousto-Optical Beam Splitter). Optical sections separated by 0.3 μm were collected and only cells with signals from both alleles were analyzed using Image J software (NIH). Alleles were defined as colocalized with γH2AX if the signals directly overlapped (at least one pixel of colocalization).

Supplemental References

Calado, D.P., Sasaki, Y., Godinho, S.A., Pellerin, A., Kochert, K., Sleckman, B.P., de Alboran, I.M., Janz, M., Rodig, S., and Rajewsky, K. (2012). The cell-cycle regulator c-Myc is essential for the formation and maintenance of germinal centers. Nat Immunol *13*, 1092-1100.
Zhou, X., Xiang, Y., and Garrard, W.T. (2010). The Igkappa gene enhancers, E3' and Ed, are essential for triggering transcription. J Immunol *185*, 7544-7552.